TITLE

Chemogenomic profiling of human and microbial FK506-binding proteins

Authors: Sebastian Pomplun[a‡], Claudia Sippel[a], Andreas Hähle[a,b], Donald Tay[c], Kensuke Shima[d], Alina Klages[e], Can Murat Ünal[e], Benedikt Rieß[a], Hui Ting Toh[c], Guido Hansen[g], Ho Sup Yoon[c], Andreas Bracher[h], Peter Preiser[c], Jan Rupp[d], Michael Steinert[d,f] and Felix Hausch[*a,b]

Affiliations:

[a]Department of Translational Research in Psychiatry, Max Planck Institute of Psychiatry, 80804 Munich, Germany

[b]Technical University Darmstadt, 64289, Darmstadt, Germany

[c]School of Biological Sciences, Nanyang Technological University, Singapore

[d]Department of Infectious Diseases and Microbiology, University of Lübeck, Lübeck, Germany

[e]Technische Universität Braunschweig, 38106 Braunschweig, Germany

[f]Helmholtz Centre for Infection Research, 38124 Braunschweig, Germany

[g]University of Lübeck, Germany

[h]Max Planck Institute of Biochemistry, 82152 Martinsried,

[‡] Current Address: Roche Diagnostics, 82377 Penzberg

Corresponding address: Felix Hausch, Technical University Darmstadt, Alarich-Weiss-Str. 4, 64287 Darmstadt, Germany. Tel +49 (6151) 16.21245, hausch@drugdiscovery.chemie.tu-darmstadt.de

Conflict of Interest: The authors declare that no conflict of interest exists

Abstract

FK506-binding proteins (FKBPs) are evolutionary conserved proteins that display peptidyl-prolyl isomerase activity and act as co-receptors for immunosuppressants. Microbial macrophage infectivity potentiator (Mip) type FKBPs can enhance infectivity. However, developing drug-like ligands for FKBPs or Mips has proven difficult and many FKBPs/Mips still lack a biologically useful ligand. To explore the scope and potential of C^5-substituted-[4.3.1]-aza-bicyclic sulfonamides as a broadly applicable class of FKBP inhibitors, we developed a new synthesis for the bicyclic core scaffold and used it to prepare a FKBP/Mip-focused library. This allowed a systematic structure-activity relationship analysis across key human FKBPs and microbial Mips, yielding highly improved inhibitors for all FKBPs studied. A co-crystal structure confirmed the molecular binding mode of the core structure and explained the affinity gain by preferred substitutents. The best FKBP/Mip ligands showed promising anti-malarial, anti-leginonella and anti-clamydial properties in cellular models of infectivity, suggesting substituted-[4.3.1]-aza-bicyclic sulfonamides as a novel class of anti-infectives.

Introduction

FK506-binding proteins (FKBPs) are part of the immunophilin family and bind the natural products FK506 (Fig. 1A) and rapamycin. They are best known for their ability to enable the immunosuppressive effects of these drugs by a remarkable gain-of-function mechanism.[1, 2] Beyond ligand-induced immunosuppression, human FKBPs have been implicated in calcium signaling[3, 4], metabolic[5, 6] or psychiatric disorders [7-9] as well as chronic pain [10, 11]. FKBPs are highly conserved and present in all kingdoms of life, including several human pathogens. Fungal FKBPs are thought to mediate the anti-fungal properties of FK506 or rapamycin by chemically inducing FKBP-protein complexes similar to the immunosuppressive mechanism in mammals[12, 13]. *Plasmodium falciparum*, the causative agent of malaria, expresses a FKBP homolog (*Pf*FKBP35) and is sensitive to FK506 and rapamycin. However, whether this sensitivity is due to the induction of protein complexes (like in other eukaryotes), due to direct inhibition of pfFKBP35, or mediated by non-FKBP proteins is unclear.[14] In addition, many Gram-negative bacteria express FKBP homologs that have been reported

to be important for virulence or replication of intra- and extracellular bacterial pathogens.[15, 16] The prototypical member of these FKBPs was first described in *Legionella pneumophila* and named macrophage infectivity potentiator (Mip) as it supports the intracellular replication of this pathogen in phagocytic cells.[17, 18]

Taken together, FKBPs are considered as promising drug targets. Traditionally, FKBPs have been studied pharmacologically using the prototypic ligands FK506 or rapamycin.[19-21] For most FKBPs, little is known regarding the recognition of ligands beyond these two natural products. FK506 potently inhibits calcineurin whereas rapamycin blocks mTOR when bound by human FKBPs, respectively. This can severely confound or even obliterate studies in more complex biological systems. Moreover, the immunosuppression associated with these drugs is clearly counterproductive for a putative anti-infective agent.

In the effort to develop binders for FKBPs, which do not interfere with the immune response, we recently identified bicycles such as **1a** as highly efficient ligands of human FKBP12, 51 and 52 (Fig. 1B).[22-24] In this scaffold, the [4.3.1]-bicycle mimics the pipecolate core of FK506 in its active conformation and presents three vectors to allow positioning of variable substituents to interact with the rim of the FK506-binding site (Fig. 1C).

The FK506-binding pockets of human, bacterial, fungal or plasmodium FKBPs are highly conserved (Fig. 1D). Motivated by the high structural similarity of the FK506 binding site across many FKBPs, we explored, whether the (*S*)-C5-substituted [4.3.1]-aza-amide bicyclic core would be a general privileged scaffold for therapeutically relevant FKBPs.

Results and Discussion

Synthesis of a FKBP/Mip-focused substance library. We first aimed to explore the role of R^1 substituents in bicyclic ligands corresponding to scaffold **1**. Towards the generation of a FKBP-focused library of R^1-derivatized 4.3.1]-aza-amide bicycles we first developed an efficient synthesis of the key precursor **7** harbouring the PMB protection group in R^1 (Fig. 2A). As the R^2-substitutent 3,5,-dichlorphenylsulfonyl was kept constant in this series, as this subgroup provided promising initial affinities for binding to human FKBP12, FKBP51 and FKBP52.[22]

The synthesis commenced with allylation of phtalimide. The resulting allyl-phtalimide **2** was transformed by metathesis with allylTMS and Grubbs 1° generation catalyst and subsequently deprotected to afford the 4-TMS-but-2-en-1-amine **4**. An E-selective synthesis for this compound is known[25] but in our case the stereochemistry of the double bond does not influence the further course of the synthesis. Reductive amination of this fragment with paramethoxybenzaldehyde resulted in the building block **5**. This was reacted with commercially available (*S*)-6-oxo-2-piperidinecarboxylic acid and subsequently Boc-protected to furnish **6**, the precursors for the key chemoselective reduction/asymmetric N-acyliminium cyclization.[24] Reduction with DIBAL-H and subsequent treatment with hydrofluoric acid in pyridine resulted in the bicyclic building block **7** in 8 g scale and 29 % yield over 8 steps. Reaction with dichlorphenyl sulfonyl chloride afforded the key intermediate **9**.

For variation of the R^1 substituent, compound **9** was deprotected with CAN. The resulting carboxamide of **10** was then alkylated with various halides to afford bicycles **11a-n** and **17a**. To further enhance the diversity in the R^1 position compounds **11d** and **11h** were further derivatized to yield compounds **11o-u** (Fig. 2B).

Preliminary results showed that a pipecolyl group in the R^1-position provided comparatively high binding to several FKBPs. We thus kept this subgroup constant in a subseries aimed to explore the R^2-group. We thus adopted the synthetic route developed above to the synthesis of the key building block

14, which was obtained in multigram scale and 20 % yield over 8 steps (Fig. 2C). Intermediate **14** was derivatized with various commercially available arylsulfonyl chlorides to yield **15a-p** and **16a**.

For the exploration of various R^3 substituents in the C^5 position, compounds **16a** and **17a** were chosen as high-affinity starting points (Fig. 3). Taking advantage of the orthogonal reactivity of the vinyl group, alkenes **16a** and **17a** were first reduced to provide the saturated analogs **16b** and **17b**. Oxidative cleavage of the vinyl group furnished aldehydes **16c** and **17c**, which were further smoothly converted to the dimethylamine **16d**, methylamine **17d**, or the carboxylic acid **17e**. Standard transformations as f follow-up provided amide **17f**, the difluoromethyl group **16e**, and the acetylene **16f**. Reduction of the aldehydes with sodium borohydride gave alcohols **16h** and **17g**, which were subsequently further transformed to the corresponding methyl ethers (**16j**, **17h**), the ethyl ether **16k** or the fluoromethyl group **16i**.

Affinity determination and profiling of FKBP/Mip proteins.

The 54 final bicyclic sulfonamides were tested for binding to six human FKBPs (FKBP12, 12.6, 13, 25, 51 and 52) and five microbial FKBPs (from *Candida albicans*, *Plasmodium falciparum*, *Chlamydia pneumonia*, *Chlamydia trachomatis*, and *Legionella pneumophila*) using a competitive fluorescence polarization assay (Tab. 1). Gratifyingly, the microbial FKBPs bound to previously developed fluorescent tracers[26] allowing rapid affinity measurements for these proteins (Tab. 1 and Suppl. Tab. 2). However, since several [4.3.1]-bicyclic sulfonamides bound very tightly to some of the human FKBPs (e.g., K_i < 0.5 nM for FKBP12) the exact affinity of these compounds could not be fully determined with the previously published assays[26].We therefore developed a more sensitive fluorescent tracer **16g** derived from the high-affinity ligand **16f** (Figure 3). Tracer **16g** tightly bound to all FKBPs including FKBP12 (K_d= 0.57 ± 0.03 nM) and FKBP12.6 (K_d= 0.53 ± 0.17 nM), allowing precise measurements of the high-affinity ligands for these proteins.

For human FKBPs, *Ca*FKBP12, *Pf*FKBP35 and *Lp*Mip, the best [4.3.1] bicycles such as **16j** (Fig. 4A) rivalled or exceeded the affinity of the prototypic ligand FK506 as well as the affinity of the best

ligands published for these proteins so far.[27-38] For *Cp*Mip, which has no characterized ligand so far, compound **11j** was found to bind substantially better than FK506.

In general, the small human FKBPs bound tighter to the [4.3.1]-bicycles compare to their larger homologs (FKBP12 > 12.6 > 13 ≈ 51 ≈ 52 >> 25). For the microbial FKBPs, the average affinities decreased from *Ca*FKBP12 > *Pf*FKBP35 >> *Cp*Mip ≈ *Lp*Mip > *Ct*Mip. This tendency of closely correlated with the sequence homology of FKBPs to human FKBP12. Whether the enhanced ligand-binding propensity of FKBP12 is restricted to compounds of scaffold **1** or intrinsic to the individual binding pockets remains to be elucidated, possibly by the investigation of alternative scaffolds or by unbiased screening of large substance libraries.[39]

The high affinities for human FKBP12 suggest that microbial FKBP inhibition in the absence of FKBP12 inhibition may be difficult. However, by using an elegant approach recently described by Nambu *et al.* potent and selective inhibition of human FKBP12 observed here can actually be turned into an advantage in an anti-fungal therapy[29]. By blocking human FKBP12, but not fungal FKBP12, e.g. with compound **16b** ($K_i^{HsFKBP12}$/ $K_i^{CaFKBP12}$= 40), FK506 can be directed to inhibit fungal calcineurin only.

Binding mode of C^5-modified [4.3.1]-bicyclic FKBP ligands.

An exemplary cocrystal structure of the FK506-binding domain of FKBP51 in complex with ligand **16h** was solved to clarify the molecular basis for the improved affinity of the optimized bicyclic ligands (Fig. 4B and Suppl. Tab. 2). The key interactions were van-der-Waals contacts of the pipecolyl ring with a hydrophobic cage formed by Tyr^{57}, Phe^{77}, Val^{86}, Ile^{87} and Trp^{90} as well as a hydrogen bond between the pipecolyl carbonyl oxygen and the amide of Ile^{87} (FKBP51 numbering). The high resolution also unambiguously defined a very short close contact (3.0Å) between the pipecolyl carbonyl carbon and the phenyl oxygen of Tyr^{113}, which likely reflects an orthogonal dipolar interaction.

For the contacts of the R^1-R^3 substituents we observed a hydrogen bond between picolinyl in R^1 and Tyr^{113} as well as a halogen bond between the R^2 aryl chlorine and Ser^{118} (Fig. 4B), structurally

explaining the preferred binding of compounds with these functional groups. The hydroxymethylene group in R^3 did not engage in direct contacts with FKBP51, possibly explaining the shallow structure-activity relationship in this position. The hydroxyl group was able to adopt two possible conformations, which interacted indirectly via water molecules with the backbone carbonyl of Gln^{85} or the side chains of Asp^{68} and Ser^{118} (Fig. 4C).

Structure-activity relationship analysis of [4.3.1]-bicyclic derivatives.

The analysis of R^1 moieties revealed that truncation of the 3-dimethoxy phenyl ether in **1a** (R^1= C_2H_4O*Ph(OMe)$_2$*) to a simple methyl ether in **17a** (R^1= C_2H_4O*Me*) only marginally compromised affinity (K_i^{FKBP12}= 8.8 ± 0.5 nM → 18.8 ± 1.8 nM). Likewise, smaller or larger substituents on the γ-oxygen were well tolerated, e.g., **11m** (R^1= C_2H_4O*H*; K_i^{FKBP12}= 11.8 ± 2.7 nM) or **11p** (R^1= C_2H_4O*Et*; K_i^{FKBP12}= 21.1 ± 1.3 nM). However, the γ-position of the ether was important since moving the oxygen to the δ-position as in **11e** (R^1= C_3H_6O*Me*; K_i^{FKBP12}= 143 ± 16 nM) or the ε-position as in **11f** (R^1= C_4H_8O*Me*; K_i^{FKBP12}= 249 ± 2 nM) substantially affected affinity. Removal of the ether group as in **10**, **11a**, **11c**, **11g** or **11q** slightly reduced affinity (K_i^{FKBP12}= 49-80 nM), whereas replacement by alternative hydrogen bond acceptors as in **11h** and **11r-u** retained it (K_i^{FKBP12}= 7-25 nM). Likewise, pyridine analogs like **11k** and **11l** (with a hydrogen bond acceptor in the ortho position) were beneficial R^1 moieties, whereas a phenyl moiety such as in **9** or five-membered heterocycles such as **11i** and **11j** were not. This analysis – discussed here for hsFKBP12 – generally hold true for most FKBPs/Mips. A notable exception was **11j** (with a furanylmethyl group), which bound comparatively well to *chlamydiae* Mips.

In the R^2 position, halogens in the meta position generally enhanced affinity compared to the unmodified phenyl sulfonyl group (**15b**). For Mips, a cyano group as in **15g** in this position appeared to be comparatively favourable. Heterocycles instead of the phenyl ring such as in **15a** and **15c** were disadvantageous but fused heterocycles such as in **15o** and **15p** tended to be favourable. Surprisingly, a pyrimidin in the para position as in **15m** was particularly beneficial for CaFKBP12 (K_i= 52 nM). The

R^3 position was generally rather tolerant to modifications, with hydroxymethyl or methoxymethyl (as in **16j**) conferring the highest affinity to FKBPs (Fig. 4A). A carboxyl group was clearly not tolerated (compare **17e** vs. **17b** or **17f**).

A general finding for all FKBPs was the absence of cooperativity effects between the R^1, R^2 and R^3 moieties. Productive interactions such as a hydrogen bond acceptor in the γ-position of R^1 or the halogen bond donor in the meta position of R^2 appear to operate independently. However, the beneficial effect of a hydrogen bond acceptor in R^1 might not extend to compounds with a carboxamides[32,33,40,41] in R^2 since in this case the Tyr^{113} (Tyr^{89} in FKBP12) hydrogen donor would already be satisfied.

Inhibition of microbial growth/proliferation: Given the promising affinities of several [4.3.1]-bicyclic sulfonamides for microbial FKBPs we characterized the effects of the most advanced compounds on microbial growth. Compound **16b** as exemplary high-affinity ligand for microbial FKBPs/Mips dose-dependently reduced parasitaemia in the *Plasmodium falciparum* strain 3D7 with an IC_{50} = 2.3µM (Fig. 5A & 5B). Similar results were obtained with the weaker *Pf*FKBP35 ligand **17b** (IC_{50} = 8.3µM; Suppl. Fig. 1B). Importantly, **16b** maintained its anti-malarial activity in the multidrug-resistant strain Dd2 (Fig. 5C).

In the past, *Lp*Mip was shown to be important for the intracellular growth of *Legionella pneumophila*, the causative agent of Legionnaires' disease.[17, 42] Accordingly, we tested the potential of [4.3.1]-bicyclic sulfonamides to inhibit the proliferation of this intracellular pathogen in human THP-1 monocytes that have been differentiated to macrophages. Compounds **16b** and **17b** abolished intracellular proliferation of the bacteria in a dose dependent manner when they were added 2 h after infection following the removal of extracellular bacteria. An anti-proliferative activity could be observed for both compounds at concentrations at ≥20 µM. This resulted in a repression of intracellular replication within the first 24 h of infection to a level comparable to the avirulent *dotA*-negative mutant (Fig. 5D and Suppl. Fig. 1C).

Next, we tested the effect of the **11j** on Chlamydia species since **11j** display high affinity for *Cp*/*Ct*Mip and discriminated at least against the large human FKBPs. Chlamydia have a unique developmental cycle that alternates between two distinct forms: infectious elementary bodies (EBs) and the metabolically more active reticulate bodies (RBs). After internalization into host cells, EBs differentiate into RBs in an intracellular membrane-bound compartment called the chlamydial inclusion for their replication. To re-infect neighboring cells, RBs revert to infectious progeny EBs prior to cell lysis. Compound **11j** led to a slightly reduced inclusion size in host cells infected with *Chlamydia pneumoniae* (Fig. 5E, bottom left). However, consistent with prior observations,[43] the generation of infectious EBs was reduced dramatically (Fig. 5E, bottom right). Similar results were also observed for *C. trachomatis* (Suppl. Fig. 1D), indicating that inhibition of Mip might principally block RB to EB conversion in Chlamydia, thereby suppressing infectivity. It is important to note, that at this point we cannot fully exclude a participation of human host FKBPs in the anti-Chlamydia or anti-Legionella effects observed. More selective inhibitors will be needed to clarify this issue.

Conclusion

Taken together, our results show that (S)-C^5-substituted-[4.3.1]-aza-amide bicyclic compounds are a privileged, broad-ranged class of FKBP inhibitors. We present the first systematic SAR analysis for human FKBP12.6, 13, and 25 and *Cp*Mip as well as the first useful inhibitor for the latter. Compounds such as **11j** or **15m** show that with carefully chosen substituents the selectivity profile can be tuned (e.g. for *Cp*/*Ct*Mips or *Ca*FKBP12). Our results suggest that the PPIase active site plays indeed a crucial role in the life cycle of *P. falciparum, L. pneumophila, C. pneumoniae, and C. trachomatis.* The presented compounds will be highly useful as probes to study FKBP/Mip function as well as starting points for the further development of FKBP/Mip-directed drugs.

.

Experimental Section

1. Organic Synthesis

General: Reactions were performed in heatgun-dried flasks under Argon atmosphere. All reagents were purchased from commercial sources and were used directly without further purification. **Nuclear Magnetic Resonance:** ^{1}H- and ^{13}C-NMR spectra were recorded at the Department of Chemistry and Pharmacy at the Ludwig-Maximilian University of Munich on a Bruker AC300, a Bruker XL400 or a Bruker AMX600 at room temperature. Chemicals shifts are reported in parts per million referenced with respect to residual solvent (^{1}H: $CDCl_3$ = 7.26 ppm, ^{13}C: $CDCl_3$ = 77.16 ± 0.06 ppm). The coupling constants (*J*) are given in Hertz (Hz) and the peak multiplicity are abbreviated as singlet (s), doublet (d), triplet (t), quartet (q) and multiplet (m). **Mass Spectrometry:** ESI mass spectra (m/z) were recorded on a Thermo Finnigan LCQ DECA XP Plus mass spectrometer. **High-Performance Liquid Chromatography:**Analytical reverse phase HPLC was performed using a Beckman System Gold 125S Analytical Solvent Module, a Beckman 168 Diode Array Detector Module, a Beckman 508 Autosampler Module with a 50 µL sampling loop, and a Jupiter 4 µm Proteo 90 Å 250 x 4.6 mm analytical column (Phenomenex, Germany) at a flow rate of 1 mL/min using buffer A: 0.1 % TFA in water/acetonitrile (95/5, v/v) and buffer B: 0.1 % TFA in acetonitrile/water (95/5, v/v). **Flash Chromatography:** Chromatographic separations were performed either manually or with an Interchim Puriflash 430 automatic flash chromatography system. Silica gel 60 (Merck 70-230 mesh) was used for manual column chromatography. Puriflash columns 50 Silica 50 µM (10 g, 25 g, and 40 g) were used for automated chromatography. **Thin Layer Chromatography:** Thin layer chromatography (TLC) was performed using Merck-preprared aluminium plates (Silica 60 F254, 0.25 mm). The substances were detected with UV-light (λ = 254/366 nm). Thin layers plates were also stained with the following solutions: Hanessian's: 5 g $CeSO_4$, 25 g $NH_4MO_7O_{24}\cdot 4\ H_2O$, 450 mL H_2O, 50 mL H_2SO_4. Potassium permanganate: 1.5 g $KMnO_4$, 10 g K_2CO_3, 1.25 mL 10 % NaOH in 200 mL H_2O. **Purity**: The purity of the compounds was verified by reversed phase HPLC. All the final compounds synthesized and tested have a purity of more than 95 %

Synthesis of 2: 2-allylisoindoline-1,3-dione

To a solution of Phtalimide (15.0 g, 102 mmol) in DMF (100 mL) were added K_2CO_3 (14.1 g, 102 mmol) and Allylbromide (12.3 g, 8.82 mL, 102 mmol). After 3 h stirring at room temperature EtO_2 (300 mL) was added to the reaction mixture and washed with sat. aq. NaCl solution (3 × 75 mL). After extraction the solvent was removed under reduced pressure affording the title compound (19.0 g, 101 mmol, 99.0 %) as a colourless solid, which was used for the next step without further purification. $\mathbf{R_f}$: 0.43 (Cyclohexane/EtOAc = 85:15) **^{1}H NMR** (300 MHz, $CDCl_3$) δ = 4.29 (dt, *J* = 5.7, 1.5 Hz, 2 H), 5.15 – 5.31 (m, 2 H), 5.79 – 5.97 (m, 1 H), 7.68 – 7.76 (m, 2 H), 7.80 – 7.89 (m, 2 H). **^{13}C-NMR** (75.5 MHz, $CDCl_3$) δ = 40.03, 117.72, 123.27, 131.50, 132.10, 133.94, 167.88.

Synthesis of 3: **2-(4-(trimethylsilyl)but-2-en-1-yl)isoindoline-1,3-dione**

To a solution of 2-allylisoindoline-1,3-dione (13.0 g, 69.4 mmol) in CH_2Cl_2 (500 mL) was added AllylTMS (79.0 g, 110 mL, 694 mmol) and Grubbs I generation catalyst (12 % loading). The reaction was heated to 60 °C and stirred under reflux for 4 h. Tris(hydrodxymethyl)phosphine (1 M solution in *i*-PrOH, 58 mL) was added and stirred under reflux for 12 h, while the color of the reaction turned from black to orange. Sat. aq. NaCl solution (100 mL) was added to the reaction and the organic phase was separated. The aqueous phase was extracted with CH_2Cl_2 (3 × 200 mL). The combined organic layers were dried over $MgSO_4$ and the solvent was removed under reduced pressure. Column chromatography over SiO_2 (Cyclohexane/ EtOAc = 85:15) afforded the title compound (15.0 g, 54.9 mmol, 78.9 %) as a yellow resin. $\mathbf{R_f}$: 0.57 (Cyclohexane/EtOAc = 85:15) **^{1}H NMR** (300 MHz, $CDCl_3$) δ = -0.10 – 0.09 (m, 9H), 1.44 (d, *J* = 8.2 Hz, 1.6 H), 1.72 (d, *J* = 8.8 Hz, 0.4 H), 4.21 (d, *J* = 6.5 Hz, 1.6 H), 4.29 (dd, *J* = 14.5, 5.9 Hz, 0.4 H), 5.26 – 5.47 (m, 0.8 H), 5.56 – 5.70 (m, 0.2 H), 5.70 – 5.87 (m, 0.8 H), 5.94 – 6.09 (m, 0.2 H), 7.65 – 7.74 (m, 2H), 7.79 – 7.88 (m, 2H).**^{13}C NMR** (75 MHz, $cdcl_3$) δ -2.05, -1.83, -1.43, 18.92, 22.73, 34.72, 39.87, 120.51, 121.30, 123.12, 130.78, 132.24, 133.76, 133.90, 167.99.

Synthesis of 4: **4-(trimethylsilyl)but-2-en-1-amine**

To a solution of 2-(4-(trimethylsilyl)but-2-en-1-yl)isoindoline-1,3-dione (150 mg, 0.549 mmol) in MeOH (5 mL) was added Hydrazine (35.2 mg, 0.034 mL, 1.10 mmol) and the reaction was heated to 75 °C and stirred under reflux for 24 h. CH_2Cl_2 (90 mL) was added to the solution and washed with NaOH (1 M solution, 3 x 10 mL). The organic layer was dried over $MgSO_4$ and the solvent was removed under reduced pressure (at room temperature at 150 mbar) affording the title compound as a colourless liquid, which was stored at – 20 °C. **R_f**: 0.24 (EtOAc + 2 % MeOH + 2% TEA) **^{1}H NMR** (300 MHz, $CDCl_3$) δ = -0.04 – 0.03 (m, 9 H), 1.40 – 1.50 (m, 2 H), 1.69 (s, 2 H), 3.14 – 3.34 (m, 2 H), 5.30 – 5.61 (m, 2 H). **^{13}C NMR** (75 MHz, $CDCl_3$) δ = -2.02, 22.50, 44.36, 127.19, 129.72.

Synthesis of 5a: N-(4-methoxybenzyl)-4-(trimethylsilyl)but-2-en-1-amine

To a solution of 4-(trimethylsilyl)but-2-en-1-amine (7.86 g, 54.8 mmol) in EtOH (250 mL) was added 4-methoxybenzaldehyde (7.47 g, 54.8 mL, 1.10 mmol). After 2h stirring at room temperature $NaBH_4$ (3.11 g, 82 mmol) was added to the solution, which was stirred until no gas evolution was observed. NaOH (1 M solution, 100 mL) was added to the reaction mixture, which was extracted with CH_2Cl_2 (300 mL). The organic layer was dried over $MgSO_4$ and the solvent was removed under reduced pressure. Column chromatography (EtOAc + 2 % MeOH + 2% TEA) afforded the title compound (11.2 g, 42.5 mmol, 77.6 % over 2 steps) as a slightly yellow oil.**R_f**: 0.35 (EtOAc + 2 % MeOH + 2% TEA) **^{1}H NMR** (600 MHz, $CDCl_3$) δ -0.24 – 0.25 (m, 9H), 1.23 (s, 1H), 1.34 – 1.46 (m, 2H), 3.13 – 3.35 (m, 2H), 3.68 – 3.81 (m, 5H), 5.52 – 5.75 (m, 1H), 6.82 – 6.89 (m, 2H), 7.20 – 7.27 (m, 2H). **^{13}C NMR** (151 MHz, $CDCl_3$) δ -1.85, 12.04, 26.30, 29.20, 52.88, 53.96, 55.23, 71.62, 113.86, 129.45, 129.80, 158.82. **MS** (ESI): *m/z* (%) = 263.98 $[M + H]^+$, 526.24 $[2M + H]^+$

Synthesis of 5b: N-(pyridin-2-ylmethyl)-4-(trimethylsilyl)but-2-en-1-amine

To a solution of 4-(trimethylsilyl)but-2-en-1-amine (13.0 g, 91.0 mmol) in EtOH (500 mL) was added picolinaldehyde (9.72 g, 91.0 mmol). After 2 h stirring at room temperature $NaBH_4$ (5.15 g, 136 mmol) was added to the solution, which was stirred until no more gas evolution was observed. $NaHCO_3$ (1 M solution, 100 mL) was added to the reaction mixture, which was extracted with CH_2Cl_2 (3 x 300 mL). The organic layer was dried over $MgSO_4$ and the solvent was removed under reduced pressure. Column chromatography (EtOAc + 3 % TEA) afforded the title compound (16.1 g, 68.7 mmol, 76 % over 2 steps) as a slightly yellow oil.

R_f: 0.3 (EtOAc + 3 % TEA) **^{1}H NMR** (300 MHz, $CDCl_3$) δ -0.03 – -0.05 (m, 9H), 1.37 – 1.50 (m, 2H), 3.19 – 3.29 (m, 2H), 3.81 – 3.91 (m, 2H), 4.73 (s, 1H), 5.32 – 5.62 (m, 2H), 7.10 – 7.20 (m, 1H), 7.24 – 7.32 (m, 1H), 7.57 – 7.69 (m, 1H), 8.50 – 8.56 (m, 1H). **^{13}C NMR** (75 MHz, $CDCl_3$) δ -1.98, -1.88, 18.92, 22.69, 45.84, 51.64, 54.35, 54.78, 64.12, 120.37, 121.79, 121.82, 122.19, 122.28, 122.29, 125.43, 126.64, 128.17, 129.34, 136.33, 136.54, 148.49, 149.23, 149.26, 159.26, 159.91, 159.94.

Synthesis of 6a.1: **(*S*)-N-(4-methoxybenzyl)-6-oxo-N-(4-(trimethylsilyl)but-2-en-1-yl)piperidine-2-carboxamide**

To a solution of (S)-6-oxopiperidine-2-carboxylic acid (1.74 g, 12.15 mmol) in DMF (120 mL) were added N-(4-methoxybenzyl)-4-(trimethylsilyl)but-2-en-1-amine (3.20 g, 12.2 mmol), EDC (2.79 g, 14.6 mmol) and HOBt (2.23 g, 14.6 mmol). After 2h stirring at room temperature Et_2O (300 mL) was added to the reaction and washed with sat. aq. NaCl solution (3 × 75 mL). The organic layer was dried over $MgSO_4$, the solvent was removed under reduced pressure and the crude title compound was used for the next step without further purification.**MS** (ESI): *m/z* (%) = 389.29 $[M + H]^+$, 777.25 $[2M + H]^+$

Synthesis of 6a: (*S*)-tert-butyl 2-((4-methoxybenzyl)(4-(trimethylsilyl)but-2-en-1-yl)carbamoyl)-6-oxopiperidine-1-carboxylate

Crude mixture of step 5 was dissolved in CH_2Cl_2 (120 mL). DIPEA (3.14 g, 4.24 mL, 24.2 mmol), Boc_2O (7.95 g, 36.4 mmol) and DMAP (1.48 g, 12.2 mmol) were added. After 24 h stirring at room temperature sat. aq. NaCl solution (25 mL) was added to the reaction and the organic phase was separated. The aqueous phase was extracted with CH_2Cl_2 (3 × 100 mL), the combined organic layers were dried over $MgSO_4$ and the solvent was removed under reduced pressure. Flash column chromatography (10 – 30 % EtOAc in Cyclohexane) afforded the title compound (3.50 g, 7.16 mmol, 59 % over two steps) as a yellow resin. **R_f**: 0.14 (Cyclohexane/EtOAc = 1:1) **^{1}H NMR** (400 MHz, $CDCl_3$) δ -0.29 – 0.22 (m, 9H), 1.38 – 1.45 (m, 2H), 1.45 – 1.54 (m, 9H), 1.70 – 1.78 (m, 1H), 1.84 – 2.06 (m, 3H), 2.36 – 2.52 (m, 1H), 2.55 – 2.67 (m, 1H), 3.69 – 3.97 (m, 5H), 4.40 – 4.63 (m, 2H), 4.96 – 5.08 (m, 1H), 5.19 – 5.36 (m, 1H), 5.52 – 5.68 (m, 1H), 6.78 – 6.92 (m, 2H), 7.12 – 7.25 (m, 2H).**^{13}C NMR** (100 MHz $CDCl_3$) δ -1.88, 18.29, 18.30, 22.89, 25.94, 26.89, 27.98, 28.01, 28.04, 28.04, 34.47, 46.98, 48.32, 55.25, 55.31, 55.66, 83.04, 113.85, 113.88, 114.22, 122.26, 122.29, 128.32, 129.37, 129.52, 129.53, 131.94, 153.32, 158.85, 170.85, 170.86, 171.39.

MS (ESI): *m/z* (%) = 389.15 $[M + H – Boc]^+$

Synthesis of 6b: **(S)-tert-butyl 2-((pyridin-2-ylmethyl)(4-(trimethylsilyl)but-2-en-1-yl)carbamoyl)piperidine-1-carboxylate**

To a solution of (S)-6-oxopiperidine-2-carboxylic acid (61.1mg, 0.427 mmol) in DMF (3 mL) were added N-(4-methoxybenzyl)-4-(trimethylsilyl)but-2-en-1-amine (100 mg, 0.427 mmol), EDC (98.0 mg , 0.512 mmol) and HOBt (78.0 mg, 0.512 mmol). After 2 h stirring at room temperature EtO_2 (90 mL) was added to the reaction mixture, which was washed with sat. aq. NaCl solution (3 × 10 mL). After extraction the organic layer was dried over $MgSO_4$, the solvent was removed under reduced pressure and the crude title compound was used for the next step without further purification. Crude (S)-N-(pyridin-2-ylmethyl)-N-(4-(trimethylsilyl)but-2-en-1-yl)piperidine-2-carboxamide (100 mg, 0.278

mmol) was dissolved in CH_2Cl_2 (3 mL). DIPEA (0.147 mL, 0.834 mmol), Boc_2O (91 mg, 0.417 mmol) and DMAP (6.80 mg, 0.056 mmol) were added. After 24 h stirring at room temperature, sat. aq. NaCl solution (10 mL) was added to the reaction and the organic phase was separated. The aqueous phase was extracted with CH_2Cl_2 (3 × 90 mL), the combined organic layers were dried over $MgSO_4$ and the solvent was removed under reduced pressure. Flash column chromatography (30 % EtOAc in Cyclohexane) afforded the title compound (90 mg, 0.195 mmol, 70 % over two steps) as a yellow resin. **R_f**: 0.26 (Cyclohexane/EtOAc = 3:7) **MS** (ESI): *m/z* (%) = 460.01 $[M + H]^+$, 360.15 $[M + H - Boc]^+$

Synthesis of 7a: (1*S*,5*R*,6*R*)-3-(4-methoxybenzyl)-5-vinyl-3,10-diazabicyclo[4.3.1]decan-2-one

A solution of (6S)-tert-butyl 2-hydroxy-6-((4-methoxybenzyl)((Z)-4-(trimethylsilyl)but-2-en-1-yl)carbamoyl)piperidine-1-carboxylate (3.5 g, 7.16 mmol) in THF (75 mL) was cooled to –78 °C and then DIBAL-H (1 M solution in CH_2Cl_2, 10.7 mL, 10.7 mmol) was added. After 15 minutes an excess of Glauber's salt (Na_2SO_4 10 H_2O) was added to the reaction. The solution was allowed to warm to room temperature and more Glaubers salt was added and stirred for 15 minutes. The solution was filtered through celite and the solvent was removed under reduced pressure, affording a yellow resin.The resin resulting from the first step was dissolved in CH_2Cl_2 (300 mL) in a teflon flask and cooled to –78 °C. HF (70 % in pyridine, 15 mL) was added and the reaction flask was transferred to an ice bath at 0 °C. After one hour, sat. aq. $CaCO_3$ solution and NaOH (10 M solution) was added to the solution to neutralize the acid and precipitate the fluoride ions as CaF_2. The reaction was extracted three times with CH_2Cl_2, the combined organic layers were dried over $MgSO_4$ and the solvent removed under reduced pressure. Column chromatography (5 % MeOH and 2 % TEA in EtOAc) afforded the title compound (1.30 g, 4.33 mmol, 60.6 % over two steps) as an orange resin.**R_f**: 0.24 (EtOAc + 2 % MeOH + 2% TEA) **^{1}H NMR** (400 MHz, $CDCl_3$) δ = 1.39 – 1.55 (m, 2 H), 1.60 – 1.65 (m, 3 H), 2.29 – 2.36 (m, 1 H), 2.40 – 2.50 (m, 1 H), 2.76 – 2.81 (m, 1 H), 2.91 (dd, *J* = 13.8, 2.0 Hz, 1 H), 3.79 (s, 3 H), 3.81 – 3.85 (m, 1 H), 3.89 (dd, *J* = 13.8, 10.8 Hz, 1 H), 4.44 (d, *J* = 14.3 Hz, 1 H),

4.73 (d, *J* = 14.3 Hz, 1 H), 4.77 – 4.91 (m, 2 H), 5.54 (ddd, *J* = 17.0, 10.2, 8.4 Hz, 1 H), 6.83 – 6.88 (m, 2 H), 7.19 – 7.25 (m, 2 H). **^{13}C NMR** (100 MHz, $CDCl_3$) δ 16.86, 28.08, 29.45, 39.05, 49.58, 50.16, 52.51, 53.01, 55.25, 57.82, 106.54, 113.90, 113.90, 115.05, 129.42, 129.82, 139.07, 149.35, 158.89, 174.64. **MS** (ESI): *m/z* (%) = 301.01 $[M + H]^+$

Synthesis of 7b: (1S,5R,6R)-3-(pyridin-2-ylmethyl)-5-vinyl-3,10-diazabicyclo[4.3.1]decan-2-one

(S)-tert-butyl 2-((pyridin-2-ylmethyl)(4-(trimethylsilyl)but-2-en-1-yl)carbamoyl)piperidine-1-carboxylate (9.8 g, 21.32 mmol) in THF (200 mL) was cooled to –78 °C and then DIBAL-H (1 M solution in CH_2Cl_2, 42.6 mL) was added. After 15 minutes an excess of Glauber's salt (Na_2SO_4 10 H_2O) was added to the reaction. The solution was allowed to warm to room temperature and more Glaubers salt was added and stirred for 15 minutes. The solution was filtered through celite and the solvent was removed under reduced pressure, affording a yellow resin. The resin resulting from the first step was dissolved in CH_2Cl_2 (800 mL) in a teflon flask and cooled to –78 °C. HF (70 % in pyridine, 40 mL) was added and the reaction flask was transferred to an ice bath at 0 °C. After one hour, sat. aq. $CaCO_3$ solution and NaOH (10 M solution) was added to the solution to neutralize the acid and to precipitate the fluoride ions as CaF_2. The reaction was extracted with CH_2Cl_2 (5 x 500 mL), the combined organic layers were dried over $MgSO_4$ and the solvent removed under reduced pressure. Column chromatography (5 % MeOH and 2 % TEA in EtOAc) afforded the title compound (2.38 g, 8.77 mmol, 40 % over two steps) as an orange resin. **^{1}H NMR** (600 MHz, $CDCl_3$) δ 1.47 – 1.53 (m, 1H), 1.59 – 1.69 (m, 4H), 1.98 – 2.05 (m, 1H), 2.25 – 2.33 (m, 1H), 2.58 – 2.65 (m, 1H), 2.78 – 2.84 (m, 1H), 3.09 (d, *J* = 13.8, 1.8 Hz, 1H), 3.83 (d, *J* = 4.0 Hz, 1H), 3.99 – 4.05 (m, 1H), 4.71 (d, *J* = 14.9 Hz, 1H), 4.81 – 4.92 (m, 3H), 5.52 – 5.60 (m, 1H), 7.14 – 7.18 (m, 1H), 7.32 (d, *J* = 7.8 Hz, 1H), 7.64 (t, *J* = 7.8, 1.8 Hz, 1H), 8.51 (d, *J* = 4.9 Hz, 1H).**^{13}C NMR** (150 MHz, $CDCl_3$) δ 16.87, 28.06, 29.36, 49.45, 51.24, 52.53, 55.90, 57.73, 115.01, 122.25, 136.68, 138.99, 149.09, 157.73, 174.91. **MS** (ESI): *m/z* (%) = 272.07 $[M + H]^+$

Synthesis of 9: **(1*S*,5*S*,6*R*)-10-((3,5-dichlorophenyl)sulfonyl)-3-(4-methoxybenzyl)-5-vinyl-3,10-diazabicyclo[4.3.1]decan-2-one**

To a solution of (1S,5S,6R)-3-(4-methoxybenzyl)-5-vinyl-3,10-diazabicyclo[4.3.1]decan-2-one (650 mg, 2.16 mmol) in CH_2Cl_2 (20 mL) were added 3,5-dichlorobenzene-1-sulfonyl chloride (1.06 g, 4.33 mmol), DMAP (264 mg, 2.16 mmol) and DIPEA (1.13 mL, 6.49 mmol) and the reaction was stirred for 16 hours at room temperature. Sat. aq. $NaHCO_3$ solution (25 mL) was added to the mixture which was extracted with CH_2Cl_2 (250 mL). The organic layer was dried over $MgSO_4$ and the solvent removed under reduced pressure. Flash column chromatography on SiO_2 (5 – 30 % EtOAc in Cyclohexane) afforded the title compound (680 mg, 1.33 mmol, 61.7 %) as a colorless solid. $\mathbf{R_f}$: 0.44 (Cyclohexane/EtOAc = 7:3) **^{1}H NMR** (400 MHz, $CDCl_3$) δ = 1.26 (d, *J* = 7.1 Hz, 2 H), 1.46 – 1.55 (m, 3 H), 2.28 – 2.41 (m, 2 H), 2.91 (dd, *J* = 14.3, 1.9 Hz, 1 H), 3.80 (s, 3 H), 3.90 (dd, *J* = 14.4, 10.9 Hz, 1 H), 3.94 – 3.98 (m, 1 H), 4.38 (d, *J* = 14.4 Hz, 1 H), 4.77 (dd, *J* = 4.2, 1.8 Hz, 1 H), 4.79 – 4.90 (m, 2 H), 5.00 (dd, *J* = 10.1, 1.3 Hz, 1 H), 5.66 (ddd, *J* = 17.0, 10.1, 8.9 Hz, 1 H), 6.86 (d, *J* = 8.8 Hz, 2 H), 7.20 (d, *J* = 8.8 Hz, 2 H), 7.54 – 7.57 (m, 1 H), 7.69 – 7.72 (m, 2 H). **^{13}C NMR** (100 MHz, $CDCl_3$) δ 15.51, 26.31, 27.58, 49.34, 50.76, 53.35, 54.82, 55.27, 56.90, 58.89, 70.66, 114.06, 116.89, 124.87, 124.97, 128.92, 129.31, 132.68, 136.32, 137.12, 144.03, 159.07, 170.19. **MS** (ESI): *m/z* (%) = 509.12 $[M + H]^+$, 1018.74 $[2M + H]^+$

Synthesis of 10: (1S,5S,6R)-10-((3,5-dichlorophenyl)sulfonyl)-5-vinyl-3,10-diazabicyclo[4.3.1]decan-2-one

To a solution of (1S,5S,6R)-10-((3,5-dichlorophenyl)sulfonyl)-3-(4-methoxybenzyl)-5-vinyl-3,10-diazabicyclo[4.3.1]decan-2-one (25.0 mg, 0.0491 mmol) in MeCN/H_2O (1.5 mL, 2:1) was added CAN (81.0 mg, 0.147 mmol). After stirring for 4 h at room temperature, sat. aq. NaCl solution (10 mL) was added to the mixture and extracted with CH_2Cl_2 (90 mL). The organic layer was dried over $MgSO_4$ and the solvent was removed under reduced pressure. Flash column chromatography on SiO_2 (10 – 40 % EtOAc in Cyclohexane) afforded the title compound (17 mg, 0.0437 mmol, 89.0 %) as a colorless

solid.**HPLC** (0-100 % B in A in 20 min): R_t = 19.16 min **R_f**: 0.16 (Cyclohexane/EtOAc = 1:1) **^{1}H NMR** (300 MHz, $CDCl_3$) δ = 1.29 – 1.36 (m, 2 H), 1.54 – 1.64 (m, 3 H), 2.23 (d, *J* = 13.0 Hz, 2 H), 2.68 (d, *J* = 7.8 Hz, 1 H), 2.90 (d, *J* = 12.5 Hz, 1 H), 3.69 – 3.85 (m, 1 H), 4.04 (s, 1 H), 4.66 (d, *J* = 5.1 Hz, 1 H), 5.06 – 5.21 (m, 2 H), 5.72 – 5.87 (m, 1 H), 7.57 (t, *J* = 1.8 Hz, 1 H), 7.70 (d, *J* = 1.8 Hz, 2 H). **^{13}C NMR** (75 MHz, $CDCl_3$) δ = 15.36, 26.48, 26.89, 26.96, 29.67, 45.07, 50.09, 55.47, 117.07, 124.89, 132.75, 136.37, 136.96, 143.97. **MS** (ESI): *m/z* (%) = 389.05 $[M + H]^+$ **HRMS**: *m/z* = 389.0508 $[M + H]^+$

Synthesis of 11j: (1S,5S,6R)-10-((3,5-dichlorophenyl)sulfonyl)-3-(furan-2-ylmethyl)-5-vinyl-3,10-diazabicyclo[4.3.1]decan-2-one

To a solution of (1S,5S,6R)-10-((3,5-dichlorophenyl)sulfonyl)-5-vinyl-3,10– diazabicyclo [4.3.1] decan-2-one (50.0 mg, 0.128 mmol) in DMF (1.0 mL) was added NaH (7.71 mg, 0.193 mmol). After 20 minutes, furfuryl chloride (29.9 mg, 0.257 mmol) was added, the solution was heated to 80 °C and stirred for 1 h. Et_2O (90 mL) was added to the solution and washed with sat. aq. NaCl solution (3 × 10 mL). The organic layer was dried over $MgSO_4$ and the solvent was removed under reduced pressure. Column chromatography on SiO_2 (Cyclohexane/EtOAc = 8:2) afforded the title compound (41.0 mg, 0.0873 mmol, 68.2 %) as a colorless solid. **HPLC** (0-100 % B in A in 20 min): R_t = 21.62 min **R_f**: 0.75 (Cyclohexane/EtOAc = 1:1) **^{1}H NMR** (600 MHz, $CDCl_3$) δ = 1.24 – 1.34 (m, 3 H), 1.48 – 1.51 (m, 2 H), 2.28 – 2.34 (m, 1 H), 2.34 – 2.42 (m, 1 H), 3.07 (dd, *J* = 14.4, 2.0 Hz, 1 H), 3.95 – 4.02 (m, 2 H), 4.25 (d, *J* = 15.2 Hz, 1 H), 4.73 (dt, *J* = 5.7, 1.8 Hz, 1 H), 4.94 – 5.08 (m, 3 H), 5.69 – 5.77 (m, 1 H), 6.27 – 6.36 (m, 2 H), 7.37 (dd, *J* = 2.0, 1.0 Hz, 1 H), 7.55 – 7.58 (m, 1 H), 7.69 (t, *J* = 1.5 Hz, 2 H). **^{13}C NMR** (150 MHz, $CDCl_3$) δ = 15.38, 26.35, 27.68, 46.59, 49.33, 50.99, 54.91, 56.92, 108.62, 110.45, 116.91, 124.86, 132.66, 136.31, 137.19, 142.31, 144.01, 150.55, 169.95. **MS** (ESI): *m/z* (%) = 469.06 $[M + H]^+$ **HRMS**: *m/z* = 469.0786 $[M + H]^+$

Synthesis of 12h: (1S,5S,6R)-10-((3,5-dichlorophenyl)sulfonyl)-5-(hydroxymethyl)-3-(pyridin-2-ylmethyl)-3,10-diazabicyclo[4.3.1]decan-2-one

To a solution of (1S,5S,6R)-10-((3,5-dichlorophenyl)sulfonyl)-3-(pyridin-2-ylmethyl)-5-vinyl-3,10-diazabicyclo[4.3.1]decan-2-one (43 mg, 0.0891 mmol) in Dioxane/H_2O (0.8 mL, 3:1) was added $NaIO_4$ (76 mg, 0.357 mmol), OsO_4 (2.5 % Solution in *tert*-Butanol, 0.00178 mmol, 0.022 mL) and 2,6-Lutidine (0.021 mL, 0.178 mmol). The solution was stirred for 24 h at room temperature, then Et_2O (90 mL) was added to the reaction, which was washed with sat. aq. NaCl solution (3 × 10 mL). The obtained crude product was dissolved in EtOH (1 mL) and $NaBH_4$ (5.00 mg, 0.132 mmol) was added and stired for 1 h at room temperature. Et_2O (90 mL) was added to the reaction and washed with sat. aq. NaCl solution (3 × 10 mL). Flash column chromatography over SiO_2 (30 – 70 % EtOAc in Cyclohexane) afforded the title compound (16 mg, 0.0330 mmol, 37.1 %) as a colorless solid. **HPLC** (0-100 % B in A in 20 min): R_t = 15.08 min **^{1}H NMR** (600 MHz, $CDCl_3$) δ = 1.24 – 1.30 (m, 2 H), 1.49 – 1.58 (m, 3 H), 2.25 – 2.33 (m, 2 H), 3.48 – 3.56 (m, 3 H), 3.86 (dd, *J* = 14.4, 10.6 Hz, 1 H), 3.92 – 3.96 (m, 1 H), 4.74 – 4.77 (m, 1 H), 4.87 (d, *J* = 7.9 Hz, 2 H), 7.29 – 7.34 (m, 1 H), 7.45 (s, 1 H), 7.56 (s, 1 H), 7.70 (s, 2 H), 7.78 – 7.83 (m, 1 H), 8.54 (dt, *J* = 5.2, 0.9 Hz, 1 H). **^{13}C NMR** (150 MHz, $CDCl_3$) δ = 15.51, 27.80, 27.82, 46.93, 49.67, 52.32, 55.22, 57.01, 63.25, 123.10, 123.22, 124.87, 132.71, 136.31, 138.63, 143.91, 147.63, 156.12, 170.54. **MS** (ESI): *m/z* (%) = 484.14 $[M + H]^+$

Synthesis of 16b: (1S,5S,6R)-10-((3,5-dichlorophenyl)sulfonyl)-5-ethyl-3-(pyridin-2-ylmethyl)-3,10-diazabicyclo[4.3.1]decan-2-one

To a solution of (1S,5S,6R)-10-((3,5-dichlorophenyl)sulfonyl)-3-(pyridin-2-ylmethyl)-5-vinyl-3,10-diazabicyclo[4.3.1]decan-2-one (35.0 mg, 0.0730 mmol) in MeOH (1 mL) was added Pd/C (10 %, 7.75 mg, 0.00729mmol) and the solution was saturated with H_2 . After 2 h, the mixture was filtered through Celite and washed with EtOAc. The solvent was removed under reduced pressure and column chromatography over SiO_2 (Cyclohexane/EtOAc = 2:3) afforded the title compound (35.1 mg, 0.0730

mmol, quant.) as a white solid. **HPLC** (0-100 % B in A in 20 min): R_t = 16.34 min **R_f:** 0.33 (Cyclohexane/EtOAc = 2:3) **^{1}H NMR (**300 MHz, $CDCl_3$**)** δ 0.78 (t, *J* = 7.4 Hz, 3H), 1.22 – 1.37 (m, 4H), 1.42 – 1.62 (m, 3H), 1.79 – 1.92 (m, 1H), 2.30 (d, *J* = 13.5 Hz, 1H), 3.11 (dd, *J* = 14.4, 1.8 Hz, 1H), 3.73 – 3.86 (m, 2H), 4.64 (d, *J* = 15.0 Hz, 1H), 4.71 – 4.77 (m, 1H), 4.93 (d, *J* = 15.0 Hz, 1H), 7.15 – 7.21 (m, 1H), 7.28 – 7.34 (m, 1H), 7.53 – 7.56 (m, 1H), 7.62 – 7.71 (m, 3H), 8.49 – 8.54 (m, 1H). **^{13}C NMR** (75 MHz, $CDCl_3$) δ 11.46, 15.62, 26.16, 27.39, 27.62, 45.56, 50.89, 55.54, 56.02, 56.90, 122.16, 122.44, 124.90, 132.57, 136.27, 136.87, 144.17, 149.13, 157.09, 170.39. **MS** (ESI): *m/z* (%) = 482.49 $[M + H]^+$ **HRMS**: *m/z* = 482.1112 $[M + H]^+$

Synthesis of 16j: (1S,5S,6R)-10-((3,5-dichlorophenyl)sulfonyl)-5-(methoxymethyl)-3-(pyridin-2-ylmethyl)-3,10-diazabicyclo[4.3.1]decan-2-one

A solution of (1S,5S,6R)-10-((3,5-dichlorophenyl)sulfonyl)-5-(hydroxymethyl)-3-(pyridin-2-ylmethyl)-3,10-diazabicyclo[4.3.1]decan-2-one (14.0 mg, 0.0290 mmol) in DMF (1 mL) was cooled to 0 °C .Then NaH (60 % dispersion in mineral oil, 2.3 mg, 0.058 mmol) was added and stirred for 20 minutes. Afterwards CH_3I (8.20 mg, 3.6 µL, 0.0.058 mmol) was added. After 16 h at room temperature, the solvent was removed under reduced pressure and column chromatography over SiO_2 (Cyclohexane/EtOAc= 3/7) afforded the title compound (8.5 mg, 0.0171 mmol, 59%) as a yellow oil. **HPLC** (0-100 % B in A in 20 min): R_t = 14.94 min**R_f**: 0.2 (Cyclohexane/EtOAc = 3:7)**^{1}H-NMR** (600MHz, $CDCl_3$) δ = 1.46 (dt, *J* = 13.3, 5.0 Hz, 1 H), 1.52 – 1.64 (m, 4 H), 2.27 – 2.33 (m, 1 H), 2.37 (dtd, *J* = 13.1, 8.6, 7.6, 5.8 Hz, 1 H), 2.88 (s, 1H), 2.95 (s, 1 H), 3.22 – 3.31 (m, 5 H), 3.76 (dd, *J* = 14.4, 10.8 Hz, 1 H), 4.00 (td, *J* = 5.0, 2.4 Hz, 1 H), 4.75 (dt, *J* = 6.2, 1.8 Hz, 1 H), 4.82 (d, *J* = 15.7 Hz, 1 H), 7.39 (s, 1 H), 7.45 – 7.51 (m, 1 H), 7.56 (d, *J* = 1.9 Hz, 1 H), 7.70 (d, *J* = 1.8 Hz, 2 H), 7.90 (t, *J* = 7.5 Hz, 1 H), 8.57 (d, *J* = 5.0 Hz, 1 H).**^{13}C-NMR** (150 MHz, $CDCl_3$) δ = 1.00, 15.50, 27.94, 28.09, 29.63, 29.66, 36.45, 44.59, 49.94, 52.68, 56.96, 59.00, 73.17, 123.17, 123.26, 124.91, 132.70, 136.27, 143.85, 170.74. **MS** (ESI): *m/z* (%) = 498.46 $[M + H]^+$ **HRMS**: *m/z* = 498.1066 $[M + H]^+$

2. Competitive fluorescence polarization assay for binding to FKBP target proteins

The competitive fluorescence polarization assay was performed according to Kozany et al.[26]. Briefly, the fluorescent tracer was diluted in assay buffer (20 mM NaCl, 20 mM HEPES pH= 8.0, 0.002% Tween20) to a concentration 1.9x of the final concentration. The competitive ligand was dissolved in DMSO to reach a 100-times diluted stock solution. This was used for a 1:1 serial dilution in DMSO. Every sample of this serial dilution was diluted by a factor of 50 in assay buffer supplemented with the fluorescent tracer to achieve a 2x concentrated mixture of fluorescent tracer and the competing ligand. 45 µl of protein at 1.11x final concentration in assay buffer were transfered in black 384-well assay plates (No.: 3575; Corning Life Sciences). 5 µl of a mixture of the fluorecent tracer and competetive ligand were added to the protein. After an incubation at room temperature for 30 min to reach equilibrium the fluorescence polarization was measured with a Tecan Genios Pro. The competition curves were analyzed by SigmaPlot 13.0.

3. Crystallography

3a) Crystallization[44]

The complex was prepared by mixing FKBP51(16-140)-A19T protein at 1.75 mM with 50 mM 12h dissolved in DMSO in a ratio of 16:1. Crystallization was performed at 20 °C using the hanging drop vapor-diffusion method, equilibrating mixtures of 1 µl protein complex and 1 µl reservoir against 500 µl reservoir solution. Crystals were obtained with reservoir solution containing 30 % PEG-3350, 0.2 M NH_4-acetate and 0.1 M HEPES-NaOH pH 7.5.

3b) Structure Solution and Refinement

The diffraction data were collected at beamline ID29 of the European Synchrotron Radiation Facility (ESRF) in Grenoble, France. Diffraction data were integrated with XDS[45], and further processed with Scala and Truncate[46], as implemented in the CCP4i. The apo structure (pdb code 3O5R) was used as a

starting point for refinement. Iterative model improvement and refinement were performed with Coot [47] and Refmac. The dictionaries for the compounds were generated with the PRODRG server[48]. Residues facing solvent channels without detectable side chain density were modeled as alanines. Molecular graphics figures were generated with the program Pymol[49]. Coordinates and structure factor amplitudes were deposited to Protein Data Bank under the accession code 5OBK.

4. Analysis of *P. falciparum* strains

4a) Cultivation and Synchronization of *P. falciparum* strains. 3D7 and Dd2 parasite cell lines were obtained from Research and Reference Reagent Resource Centre (MR4). Parasites were grown in vitro with human red blood cells obtained via the National University Hospital Blood Donation Centre, Singapore, and maintained with complete medium comprising of 16.2 g RPMI (Gibco, Life Technologies), 5 g Albumax II (Gibco, Life Technologies), 2.3 g Sodium Bicarbonate (Sigma), 0.05 g Hypoxanthine (Sigma), and 10 mg Gentamicin (Gibco, Life Technologies) per liter. Cultures were grown in 75 cm2 flasks at 2% hematocrit in a 50 mL volume. Cultures were gased with a mixed composition of 3% O_2, 5% CO_2, balanced with N_2 (Air Liquide Singapore). Late stage parasites were obtained by purification using 68% Percoll in incomplete RPMI (MP Biomedicals) density centrifugation, followed by synchronization with 5% sorbitol (Sigma) to obtain only the early post-invasion parasites.

4b) Dose Response Assay in *P. falciparum* parasite strains. Parasitemia was determined by counting the percentage of infected erythrocytes in at least 1000 cells. For each assay, the parasitemia was adjusted to 1% using uninfected erythrocytes. 100uL per well of 2% hematocrit culture were treated with a serial dilution of SP compounds dissolved in DMSO, and incubated for 60 hours. DMSO content per well did not exceed 0.05%. Each dose treatment was done in triplicates.

4c) Growth Inhibition Assay of *P. falciparum* parasite strains: Following incubation, culture supernatant was removed, and cells were resuspended in 1X Phosphate Buffered Saline (PBS) containing 16.2µM Hoechst 33342 (ThermoFisher Scientific). Staining was done for 20min at room

temperature, and was stopped by adding 200uL of 1X PBS. Parasitemia of stained treated cells were measured by Flow Cytometry using the BD Fortessa X20. Parasitemia of treated cultures were used to plot the dose response curves and estimate efficacy in the parasite strains using the ICE estimator online software tool (http://www.antimalarial-icestimator.net/MethodIntro.htm).

5. Analysis of antiproliferative activity of inhibitors on *Legionella pneumophilia*:

Determining the minimal inhibitory concentration on *L. pneumophila* and the in vitro activity of [4.3.1]-bicyclic sulfonamides in *Legionella*-infected macrophages *L. pneumophila* strain Corby were grown in YEB medium (10 g/L yeast extract, 10 g/L ACES, pH 6.9 with 10 M KOH, supplemented with 0.4 g/L L-cysteine and 0,25 g/L Fe(III)pyrophosphate) or BCYE agar (10 g/L yeast extract, 10 g/L ACES, pH 6.9 with 10 M KOH, 15 g/L agar, supplemented after autoclaving with 0.4 g/L L-cysteine and 0.25 g/L Fe(III)nitrate). When necessary, kanamycin with a final concentration of 25 µg/mL was added. Bacteria were cultured overnight at 37°C and 200 rpm, and adjusted to 2 × 107 cells/mL with YEB. One hundred microliter aliquots of these bacterial suspensions were transferred to 96 well plates and were mixed with an additional 100 µL medium with and without several [4.3.1]-bicyclic sulfonamide derivatives in a concentration range between 200 µM and 1.56 µM. Bacteria were cultured at 37°C and 180 rpm for 2 days, and growth was measured at 600 nm in a microplate reader. The human monocyte cell line THP-1 (ACC 16) was purchased from the German Collection of Microorganisms and Cell Cultures (The Leibniz Institute DSMZ), and maintained in RPMI supplemented with 10% FBS and 2 mM L-glutamine at 37°C in a 5% CO_2-atmosphere. For infection assays, the monocytes were adjusted to 5×10^5 cells/ml in fresh medium supplemented with 100 nM phorbol-12-myristate-13-acetate (PMA, Sigma–Aldrich P8139). Two hundred microliters of this suspension were transferred into the wells of a 96-well cell culture plate, and the cells were differentiated for 2 days into macrophage-like cells. For infection, *L. pneumophila* Corby was grown on BCYE agar for 3 days at 37 °C, resuspended in 1 ml of PBS, and adjusted to 10^6 cfu/ml in fresh RPMI (infection medium). The medium of differentiated THP-1 cells was replaced by 100 µL of infection medium (multiplicity of infection of 1). After 2 h, extracellular bacteria were removed by

washing three times with pre-warmed PBS. Finally, the cells were covered with fresh medium containing compound **16b** (or **17b**) derivatives at the indicated concentrations. Medium containing only 1% (v/v) DMSO was used as control. Uptake of bacteria and bacterial replication were monitored by lysing the cells after 2 and 24 h after infection, respectively, by adding Triton X-100 at a final concentration of 0.1% (v/v), and plating out serial dilutions on BCYE agar plates. After 3-4 days at 37 °C the colony forming units (cfu) were counted and related to the volume of the infection.

6. Analysis of *Chlamydia* strains

6a) Recovery assay of *Chlamydia* strains. Total of $3.5x10^4$ HEp-2 or HeLa cells in 100 µL RPMI1640 medium supplemented with 5% fetal bovine serum (FBS) (Invitrogen), non-essential amino acids (Gibco/Thermo Fischer Scientific, Waltham, MA) and 2 mM glutamine (Lonza, Walkersville, MD) were seeded into 96-well plates (Greiner bio-one, Frickenhausen, Germany) and cultured overnight at 37˚C under 5% CO_2 atmosphere. The inhibitor was added at the time of infection. Cells were infected with *C. pneumoniae* CWL029 and *C. trachomatis* serovar D of 0.2 and 0.5 IFUs/cell, respectively. The plate was further centrifuged at 700 x *g* for 1 h at 35˚C and incubated for 48 h. Afterwards, infection was analyzed by immunofluorescence staining with mouse anti-chlamydial LPS antibody (Green) which visualized chlamydial inclusions (Keyence BZ9000, Osaka, Japan). Evans blue counterstaining of host cells (red) was used for counting cell numbers. The numbers of recoverable *C. pneumoniae* and *C. trachomatis* at the indicated time points were normalized to those of the untreated controls.

6b) Statistics. Data are indicated as mean± standard deviation (SD). Statistical analysis was performed by Excel software. Data were evaluated using Student's t-test. P-values ≤ 0.05 were considered as statistically significant.

Abbreviations

DMF = *N*,*N*-Dimethylformamide; TMS = trimethylsilane; HOBt = Hydroxybenzotriazole; Boc = *tert*-butyloxycarbonyl; DIPEA = *N*,*N*-Diisopropylethylamine; DMAP = 4-Dimethylaminopyridine; DIBAL = Diisobutylaluminum hydride; THF = tetrahydrofuran; CAN = ceric ammonium nitrate; DAST = Diethylaminosulfur trifluoride; DMP = Dess Martin Periodinane; STAB = Sodium triacetoxyborohydride; TBTA = Tris(benzyltriazolylmethyl)amine.

Acknowledgements: This work was supported by the M4 Awards 2011 and 2015 from the StMWIVT (3662a/89/6 and BIO-1601-0003 to FH). We are indebted to Mrs. E. Weyher and Dr. S. Uebel (MPI of Biochemistry) for the HRMS measurement and to Mrs. C. Dubler and Dr. D. Stephenson (Ludwig-Maximilians University of Munich) for NMR measurements and the JSBG staff at the European Synchrotron Radiation Facility (ESRF) in Grenoble, France. We thank Michael Trzoss (Amplyx Pharmaceuticals, San Diego, CA) for providing a sample of CaFKBP12. AH is supported by the Hanns-Seidel-Stiftung and MS is funded by the DFG grant STE 838/8-1.

Ancillary information

Further experimental details (Suppl. Fig. 1, Suppl. Tab. 1 & 2, crystallograhic data collection and refinement statistics, NMR spectra, biological, biochemical and synthetic procedures of all compounds) are provided in the Supporting Information. Authors will release the atomic coordinates for FKBP51 (16-140)-A19T in complex with **16h** upon article publication (pdb code 5OBK). Corresponding address: Felix Hausch, Technical University Darmstadt, Alarich-Weiss-Str. 4, 64287 Darmstadt, Germany. Tel +49 (6151) 16.21245, hausch@drugdiscovery.chemie.tu-darmstadt.de

References:

1. Crabtree, G. R.; Schreiber, S. L. Three-part inventions: intracellular signaling and induced proximity. *Trends Biochem Sci* **1996,** *21*, 418-422.

2. Gaali, S.; Gopalakrishnan, R.; Wang, Y.; Kozany, C.; Hausch, F. The chemical biology of immunophilin ligands. *Curr Med Chem* **2011,** *18*, 5355-5379.

3. Gonano, L. A.; Jones, P. P. FK506-binding proteins 12 and 12.6 (FKBPs) as regulators of cardiac Ryanodine Receptors: Insights from new functional and structural knowledge. *Channels (Austin)* **2017,** *11*, 415-425.

4. MacMillan, D. FK506 binding proteins: cellular regulators of intracellular Ca2+ signalling. *Eur J Pharmacol* **2013,** *700*, 181-193.

5. Georgia Balsevich, A. S. H., Carola W. Meyer, Stoyo Karamihalev, Xixi Feng, Max L. Pöhlmann, Carine Dournes, Andres Uribe, Sara Santarelli, Christiana Labermaier, Kathrin Hafner, Michaela Breitsamer, Marily Theodoropoulou, Christian Namendorf, Manfred Uhr, Marcelo Paez-Pereda, Gerhard Winter, Felix Hausch, Alon Chen, Matthias H. Tschöp, Theo Rein, Nils C. Gassen, Mathias V. Schmidt. Stress-responsive FKBP51 is a novel regulator of metabolic function and AKT2-AS160 signaling. *Nat Commun* **2017**, *8*, 1725.

6. Stechschulte, L. A.; Qiu, B.; Warrier, M.; Hinds, T. D., Jr.; Zhang, M.; Gu, H.; Xu, Y.; Khuder, S. S.; Russo, L.; Najjar, S. M.; Lecka-Czernik, B.; Yong, W.; Sanchez, E. R. FKBP51 null mice are resistant to diet-induced obesity and the PPARgamma agonist rosiglitazone. *Endocrinology* **2016,** *157*, 3888-3900.

7. Schmidt, M. V.; Paez-Pereda, M.; Holsboer, F.; Hausch, F. The prospect of FKBP51 as a drug target. *ChemMedChem* **2012,** *7*, 1351-1359.

8. Storer, C. L.; Dickey, C. A.; Galigniana, M. D.; Rein, T.; Cox, M. B. FKBP51 and FKBP52 in signaling and disease. *Trends Endocrinol Metab* **2011,** *22*, 481-490.

9. Hausch, F. FKBPs and their role in neuronal signaling. *Biochim Biophys Acta* **2015,** *1850*, 2035-2040.

10. Maiaru, M.; Tochiki, K. K.; Cox, M. B.; Annan, L. V.; Bell, C. G.; Feng, X.; Hausch, F.; Geranton, S. M. The stress regulator FKBP51 drives chronic pain by modulating spinal glucocorticoid signaling. *Sci Transl Med* **2016,** *8*, 325ra19.

11. Maiarù, M.; Morgan, O. B.; Mao, T.; Breitsamer, M.; Bamber, H.; Pöhlmann, M.; Schmidt, M. V.; Winter, G.; Hausch, F.; Géranton, G. M. The stress regulator FKBP51: a novel and promising druggable target for the treatment of persistent pain states across sexes. *Pain* **2018**, DOI 10.1097/j.pain.0000000000001204.

12. Bastidas, R. J.; Shertz, C. A.; Lee, S. C.; Heitman, J.; Cardenas, M. E. Rapamycin exerts antifungal activity in vitro and in vivo against Mucor circinelloides via FKBP12-dependent inhibition of Tor. *Eukaryot Cell* **2012,** *11*, 270-281.

13. Juvvadi, P. R.; Lee, S. C.; Heitman, J.; Steinbach, W. J. Calcineurin in fungal virulence and drug resistance: Prospects for harnessing targeted inhibition of calcineurin for an antifungal therapeutic approach. *Virulence* **2017,** *8*, 186-197.

14. Monaghan, P.; Leneghan, D. B.; Shaw, W.; Bell, A. The antimalarial action of FK506 and rapamycin: evidence for a direct effect on FK506-binding protein PfFKBP35. *Parasitology* **2017,** *144*, 869-876.

15. Unal, C. M.; Steinert, M. Microbial peptidyl-prolyl cis/trans isomerases (PPIases): virulence factors and potential alternative drug targets. *Microbiol Mol Biol Rev* **2014,** *78*, 544-71.

16. Rasch, J.; Unal, C. M.; Steinert, M. Peptidylprolyl cis-trans isomerases of Legionella pneumophila: virulence, moonlighting and novel therapeutic targets. *Biochem Soc Trans* **2014,** *42*, 1728-1733.

17. Cianciotto, N. P.; Eisenstein, B. I.; Mody, C. H.; Toews, G. B.; Engleberg, N. C. A Legionella pneumophila gene encoding a species-specific surface protein potentiates initiation of intracellular infection. *Infect Immun* **1989,** *57*, 1255-1262.

18. Fischer, G.; Bang, H.; Ludwig, B.; Mann, K.; Hacker, J. Mip protein of Legionella pneumophila exhibits peptidyl-prolyl-cis/trans isomerase (PPIase) activity. *Molecular Microbiology* **1992,** *6*, 1375-1383.

19. Blackburn, E. A.; Walkinshaw, M. D. Targeting FKBP isoforms with small-molecule ligands. *Curr Opin Pharmacol* **2011,** *11*, 365-371.

20. Feng, X.; Pomplun, S.; Hausch, F. Recent progress in FKBP ligand development. *Curr Mol Pharmacol* **2016,** *9*, 27-36.

21. Dunyak, B. M.; Gestwicki, J. E. Peptidyl-Proline Isomerases (PPIases): Targets for natural products and natural product-inspired compounds. *J Med Chem* **2016,** *59*, 9622-9644.

22. Wang, Y.; Kirschner, A.; Fabian, A. K.; Gopalakrishnan, R.; Kress, C.; Hoogeland, B.; Koch, U.; Kozany, C.; Bracher, A.; Hausch, F. Increasing the efficiency of ligands for FK506-binding protein 51 by conformational control. *J Med Chem* **2013,** *56*, 3922-3935.

23. Bischoff, M.; Sippel, C.; Bracher, A.; Hausch, F. Stereoselective construction of the 5-hydroxy diazabicyclo[4.3.1]decane-2-one scaffold, a privileged motif for FK506-binding proteins. *Org Lett* **2014,** *16*, 5254-5257.

24. Pomplun, S.; Wang, Y.; Kirschner, A.; Kozany, C.; Bracher, A.; Hausch, F. Rational design and asymmetric synthesis of potent and neurotrophic ligands for FK506-binding proteins (FKBPs). *Angew Chem Int Ed Engl* **2015,** *54*, 345-348.

25. Tietze, L. F.; Thede, K.; Schimpf, R.; Sannicolo, F. Enantioselective synthesis of tetrahydroisoquinolines and benzazepines by silane terminated Heck reactions with the chiral ligands (+)-TMBTP and (R)-BITIANP. *Chem Comm* **2000**, 7, 583-584.

26. Kozany, C.; Marz, A.; Kress, C.; Hausch, F. Fluorescent probes to characterise FK506-binding proteins. *Chembiochem* **2009,** *10*, 1402-1410.

27. Pomplun, S.; Wang, Y.; Kirschner, A.; Kozany, C.; Bracher, A.; Hausch, F. Rationales Design und asymmetrische Synthese potenter neuritotropher Liganden für FK506-bindende Proteine (FKBPs). *Angew Chem* **2015,** *127*, 352-355.

28. Gaali, S.; Kirschner, A.; Cuboni, S.; Hartmann, J.; Kozany, C.; Balsevich, G.; Namendorf, C.; Fernandez-Vizarra, P.; Sippel, C.; Zannas, A. S.; Draenert, R.; Binder, E. B.; Almeida, O. F.; Ruhter, G.; Uhr, M.; Schmidt, M. V.; Touma, C.; Bracher, A.; Hausch, F. Selective inhibitors of the FK506-binding protein 51 by induced fit. *Nat Chem Biol* **2015,** *11*, 33-37.

29. Nambu, M.; Covel, J. A.; Kapoor, M.; Li, X.; Moloney, M. K.; Numa, M. M.; Soltow, Q. A.; Trzoss, M.; Webb, P.; Webb Ii, R. R.; Mutz, M. A calcineurin antifungal strategy with analogs of FK506. *Bioorganic & Medicinal Chemistry Letters* **2017,** *27*, 2465-2471.

30. Harikishore, A.; Leow, M. L.; Niang, M.; Rajan, S.; Pasunooti, K. K.; Preiser, P. R.; Liu, X.; Yoon, H. S. Adamantyl derivative as a potent inhibitor of plasmodium FK506 binding protein 35. *ACS Medicinal Chemistry Letters* **2013,** *4*, 1097-1101.

31. Harikishore, A.; Niang, M.; Rajan, S.; Preiser, P. R.; Yoon, H. S. Small molecule plasmodium FKBP35 inhibitor as a potential antimalaria agent. *Sci. Rep.* **2013,** *3*, 2501.

32. Seufert, F.; Kuhn, M.; Hein, M.; Weiwad, M.; Vivoli, M.; Norville, I. H.; Sarkar-Tyson, M.; Marshall, L. E.; Schweimer, K.; Bruhn, H.; Rosch, P.; Harmer, N. J.; Sotriffer, C. A.; Holzgrabe, U. Development, synthesis and structure-activity-relationships of inhibitors of the macrophage infectivity potentiator (Mip) proteins of Legionella pneumophila and Burkholderia pseudomallei. *Bioorg Med Chem* **2016,** *24*, 5134-5147.

33. Juli, C.; Sippel, M.; Jager, J.; Thiele, A.; Weiwad, M.; Schweimer, K.; Rosch, P.; Steinert, M.; Sotriffer, C. A.; Holzgrabe, U. Pipecolic acid derivatives as small-molecule inhibitors of the Legionella MIP protein. *J Med Chem* **2011,** *54*, 277-283.

34. Rasch, J.; Theuerkorn, M.; Unal, C.; Heinsohn, N.; Tran, S.; Fischer, G.; Weiwad, M.; Steinert, M. Novel cycloheximide derivatives targeting the moonlighting protein mip exhibit specific antimicrobial activity against legionella pneumophila. *Front Bioeng Biotechnol* **2015,** *3*, 41.

35. Bizzarri, M.; Tenori, E.; Martina, M. R.; Marsili, S.; Caminati, G.; Menichetti, S.; Procacci, P. New perspective on how and why immunophilin FK506-related ligands work. *The Journal of Physical Chemistry Letters* **2011,** *2*, 2834-2839.

36. Martina, M. R.; Tenori, E.; Bizzarri, M.; Menichetti, S.; Caminati, G.; Procacci, P. The precise chemical–physical nature of the pharmacore in FK506 binding protein pnhibition: ElteX, a new class of nanomolar FKBP12 ligands. *Journal of Medicinal Chemistry* **2013,** *56*, 1041-1051.

37. Feng, X.; Sippel, C.; Bracher, A.; Hausch, F. Structure−affinity relationship analysis of selective FKBP51 ligands. *J Med Chem* **2015,** 58, 7796−7806.

38. Gaali, S.; Feng, X.; Hähle, A.; Sippel, C.; Bracher, A.; Hausch, F. Rapid, structure-based exploration of pipecolic acid amides as novel selective antagonists of the FK506-binding protein 51. *J Med Chem* **2016,** 59, 2410−2422.

39. To the best of our knowledge, no validated hits have emerged publicly from high-throughut screening campains for human FKBP12, human FKBP51 or any other FKB/Mip so far.

40. Gopalakrishnan, R.; Kozany, C.; Wang, Y.; Schneider, S.; Hoogeland, B.; Bracher, A.; Hausch, F. Exploration of pipecolate sulfonamides as binders of the FK506-binding proteins 51 and 52. *J Med Chem* **2012,** *55*, 4123-4131.

41. Gopalakrishnan, R.; Kozany, C.; Gaali, S.; Kress, C.; Hoogeland, B.; Bracher, A.; Hausch, F. Evaluation of synthetic FK506 analogues as ligands for the FK506-binding proteins 51 and 52. *J Med Chem* **2012,** *55*, 4114-4122.

42. Wintermeyer, E.; Ludwig, B.; Steinert, M.; Schmidt, B.; Fischer, G.; Hacker, J. Influence of site specifically altered Mip proteins on intracellular survival of Legionella pneumophila in eukaryotic cells. *Infect Immun* **1995,** *63*, 4576-4583.

43. Reimer, A.; Seufert, F.; Weiwad, M.; Ebert, J.; Bzdyl, N. M.; Kahler, C. M.; Sarkar-Tyson, M.; Holzgrabe, U.; Rudel, T.; Kozjak-Pavlovic, V. Inhibitors of macrophage infectivity potentiator-like PPIases affect neisserial and chlamydial pathogenicity. *Int J Antimicrob Agents* **2016,** *48*, 401-8.

44. Bracher, A.; Kozany, C.; Thost, A. K.; Hausch, F. Structural characterization of the PPIase domain of FKBP51, a cochaperone of human Hsp90. *Acta Crystallogr D Biol Crystallogr* **2011,** *67*, 549-559.

45. Kabsch, W. Xds. *Acta Crystallogr D Biol Crystallogr* **2010,** *66*, 125-132.

46. French, G. S.; Wilson, K. S. On the treatment of negative intensity observations. *Acta Crystallogr. A* **1978,** *34*, 517-525.

47. Emsley, P.; Cowtan, K. Coot: model-building tools for molecular graphics. *Acta Crystallogr D Biol Crystallogr* **2004,** *60*, 2126-2132.

48. Schuttelkopf, A. W.; van Aalten, D. M. PRODRG: a tool for high-throughput crystallography of protein-ligand complexes. *Acta Crystallogr D Biol Crystallogr* **2004,** *60*, 1355-1363.

49. Delano, W. L. *The Pymol Molecular Graphics System* **2002**, www.pymol.org.

Table 1 and Figures 1-5

Table 1. Binding of [4.3.1]bicyclic ligands to human and parasite FKBPs

				FKBP/Mip										
No	**R^1**	**R^2**	**R^3**	**12**	**12.6**	**13**	**25**	**51**	**52**	***Ca*12**	***Pf*35**	***Cp*Mip**	***Ct*Mip**	***Lp*Mip**
	FK506													
	SAFit1													
1a	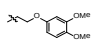													
9	PMB													
10	H													
11a	Me													
11b	*i*-Pr													
11c														
11e														
11f														
11g														
11h														
11i														
11j														
11k														

11l				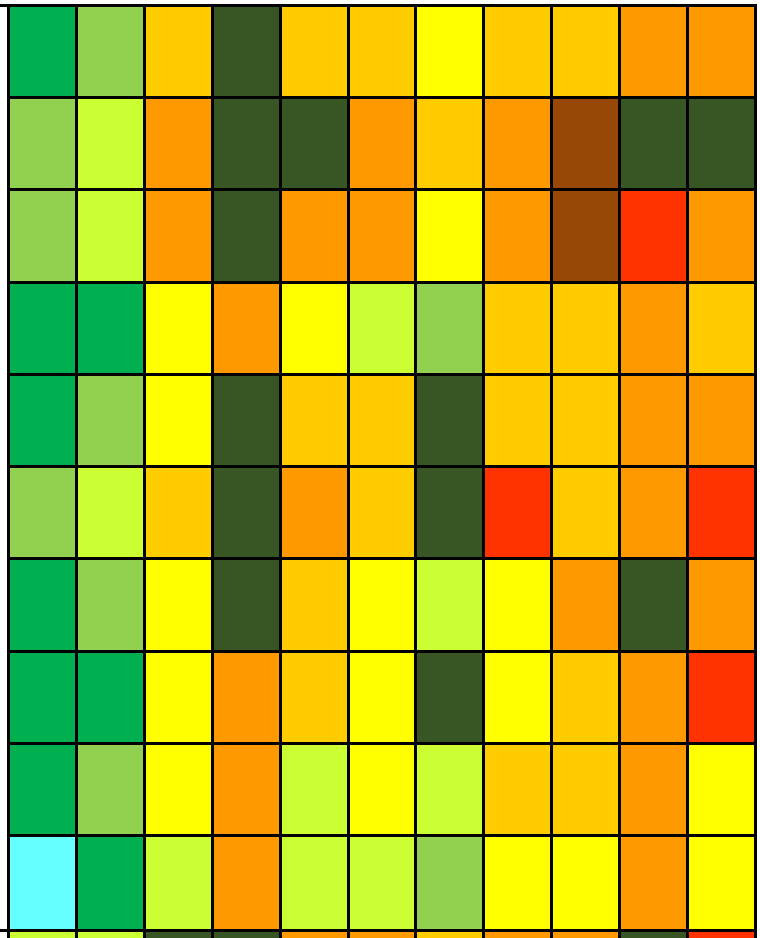
11m				
11n				
11o				
11p				
11q				
11r				
11s				
11t				
11u				
15a				
15b				
15c				
15d				
15e				
15f				
15g				
15h				
15i				

15j				
15k				
15l				
15m				
15n				
15o				
15p				
16b	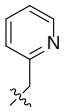			
16d				
16e				
16f				
16h				
16i				
16j				
16k				
17a				
17b				
17d				
17e				

17f														
17g														
17h														

K_i: **≤1** **-3** **-10** **-30** **-100** **0.1-0.3** **-1** **-3** **-10** **-30** **-100** **>100µM**

----------nM---------- ----------µM----------

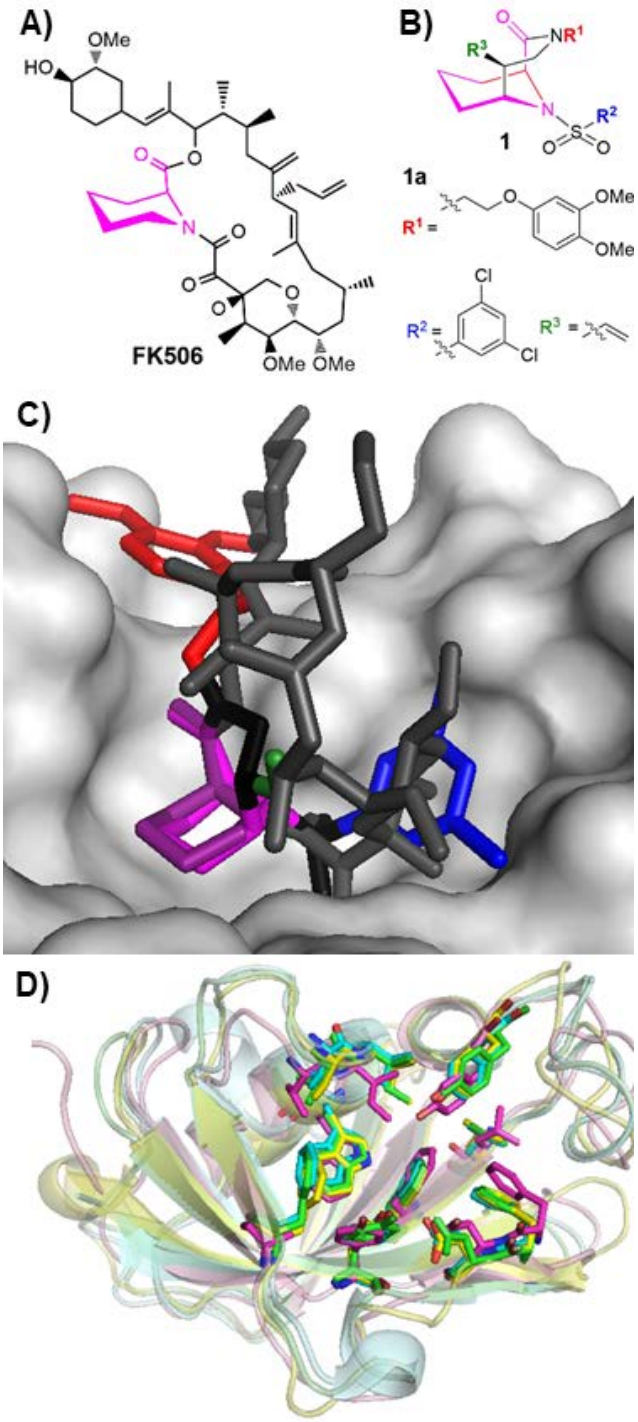

Figure 1: Structures of FKBPs and FKBP ligands. A) Chemical structures of FK506. B) Chemical structure of the (S)-C5-substituted [4.3.1]-aza-amide bicycle **1**. The pipecolate core common to FK506 and scaffold **1** is highlighted in pink.[24] C) Overlay of **1a** (from the cocrystal structure 4W9Q) on the cocrystal structure of FK506 (grey and deep purple sticks) with FKBP51 (light grey surface, pdb-code:

3O5R, Phe[77] as been omitted for clarity). The core of **1a** is highlighted as pink sticks, the three substituents are colored red, blue and green. D) FKBP12-homologous domains from human (FHBP12, green, pdb: 1FKF), *Candida albicans* (CaFKBP12, cyan, pdb: 5HW8), *Plasmodium falciparum* (pfFKBP35, yellow, pdb: 4qt3) and *Legionella pneumophila* (pfMip, magenta, pbd: 2vcd) have been superimposed. The strictly conserved residues of the FK506-binding sites are highlighted as sticks. Bound ligands (FK506 for HsFKBP12, CaFKBP12 and PfFKBP35 and rapamycin for LpMip) have been removed for clarity.

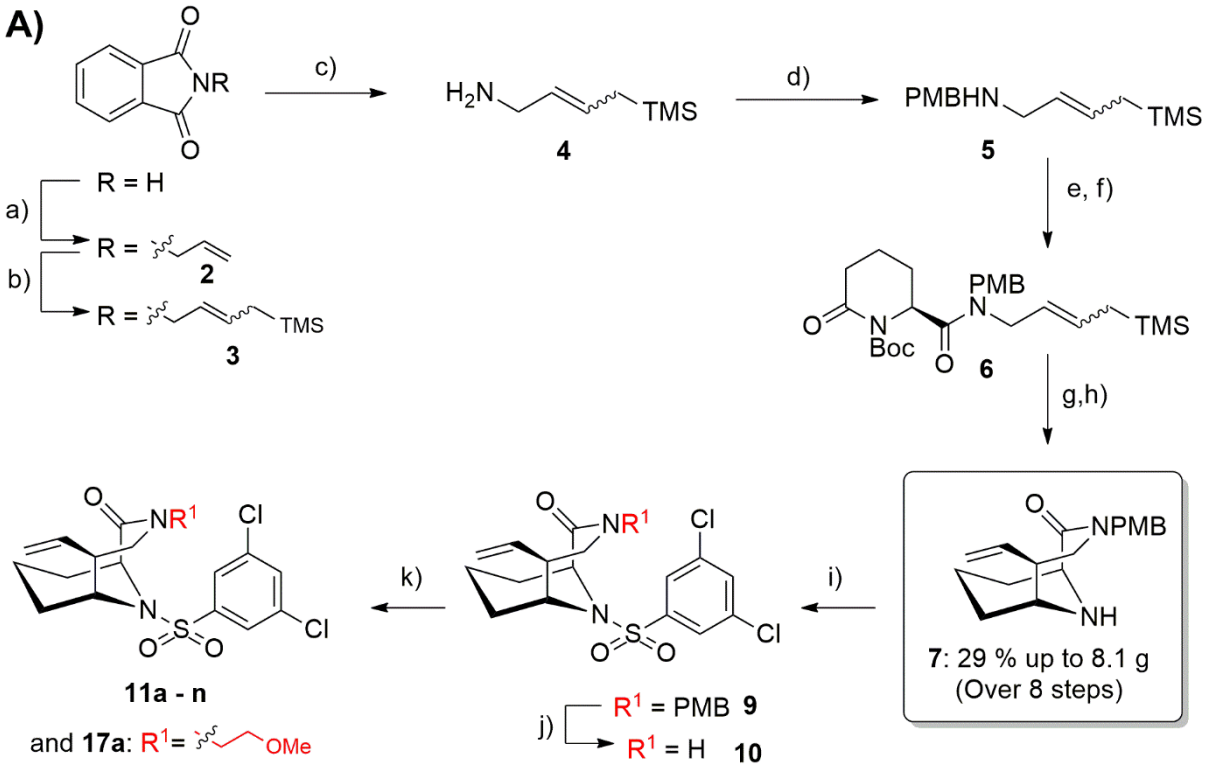
A)
R = H
a)
R =
2
b)
R =
TMS
3
c)
H2N
TMS
4
d)
PMBHN
TMS
5
e, f)
PMB
N
Boc
O
TMS
6
g,h)
NPMB
NH
7: 29 % up to 8.1 g
(Over 8 steps)
i)
NR1
Cl
N
S
O
Cl
j)
R1 = PMB 9
R1 = H 10
k)
11a - n
and 17a: R1= OMe

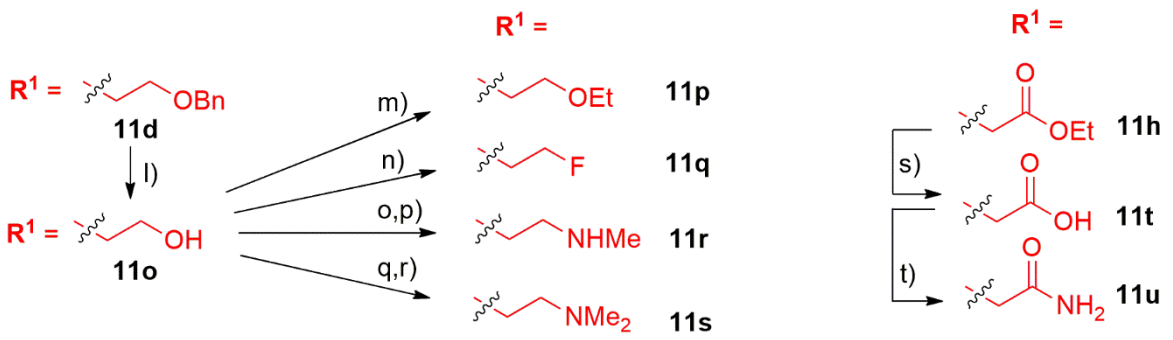
B)
R1 =
OBn
11d
l)
OH
11o
m)
n)
o,p)
q,r)
OEt
11p
F
11q
NHMe
11r
NMe2
11s
s)
11h
11t
t)
NH2
11u

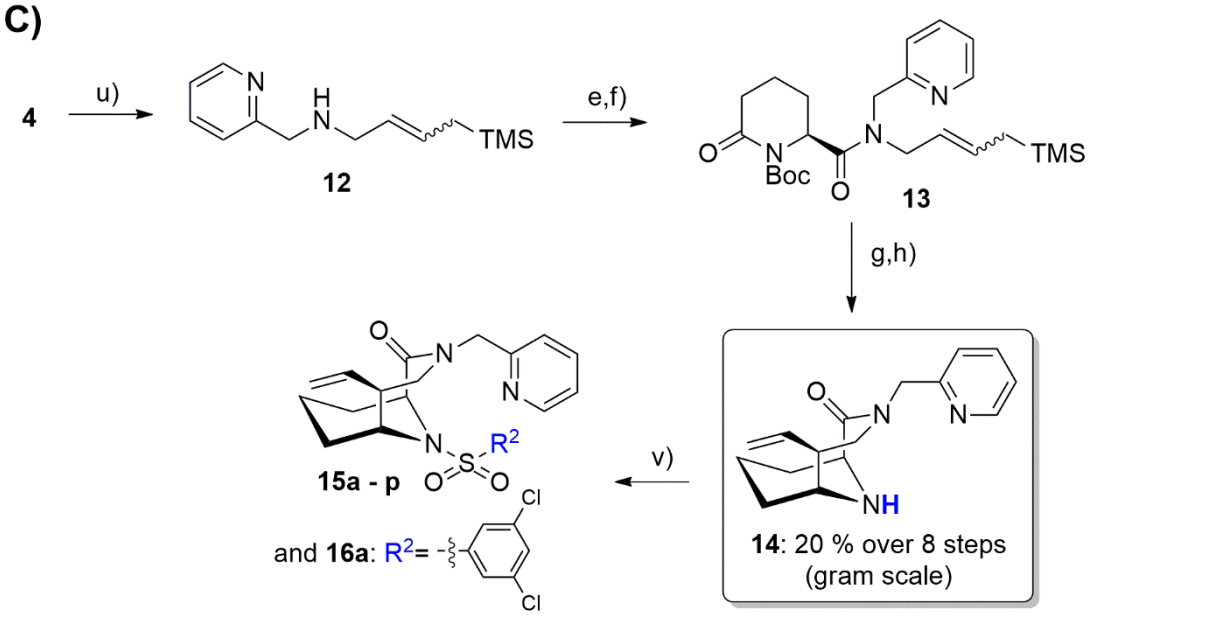
C)
4
u)
N
H
N
TMS
12
e,f)
N
N
Boc
O
TMS
13
g,h)
NH
14: 20 % over 8 steps
(gram scale)
v)
N
R2
15a - p
and 16a: R2=
Cl

Figure 2. Synthesis of the library of (S)-C5-vinyl [4.3.1]-aza-amide bicycles

A) Synthesis of the key intermediate and variation of the R^1 group. B) Follow-up derivatization the R^1 positions. C) Synthesis of derivatives with variations in the R^2 position. Reaction conditions: a) K_2CO_3, allylbromide, DMF, rt, 3 h, quant.; b) AllylTMS, Grubbs I, CH_2Cl_2, 60 °C, 4 h, 93 %; c) NH_2NH_2, MeOH, 70 °C, 24 h; d) 4-Methoxybenzaldehyde, $NaBH_4$, EtOH, rt, 4 h, 88 % (2 steps); e) (S)-6-Oxopiperidine-2-carboxylic acid, HOBt, EDC, rt, DMF, 2h; f) Boc_2O, DIPEA, DMAP, CH_2Cl_2, 48 h, 70 % (**6**), 59 % (**13**), (2 steps); g) DIBAL, THF, –78 °C, 15 min; h) HF·pyridine, CH_2Cl_2, –78 °C, 1 h, 60 % (**7**), 41 % (**14**), (2 steps); i) 3,5-dichlorobenzene-1-sulfonyl chloride, DIPEA, DMAP, rt, 24 h, 60 %; j) CAN, MeCN/H_2O, rt, 4 h, 90 %; k) NaH, R^1X, DMF, 80 °C, 1 h; l) BCl_3, CH_2Cl_2, rt, 1h, 73%; m) NaH, EtI, THF, 0°C - rt, 1h, 50 %. n) DAST, CH_2Cl_2, rt, 1 h, 52 %; o) DMP, CH_2Cl_2, 30 min, rt, 84 %; p) NH_2Me, AcOH, MeOH, STAB, rt, 2h, 39 %; q) DMP, CH_2Cl_2, 30 min, rt, 84 %; r) $NHMe_2$, $NaBH_4$, MeOH, 24 h, rt, 35 %; s) NaOH, THF/H_2O, rt, 20 h, 99 %; t) CDI, NH_3, EtOAc, rt, 90 min, 77 %; u) Picolinaldehyde, $NaBH_4$, EtOH, rt, 4 h, 76 %, (2 steps); v) R^2SO_2Cl, DIPEA, DMAP, rt, 24 h.

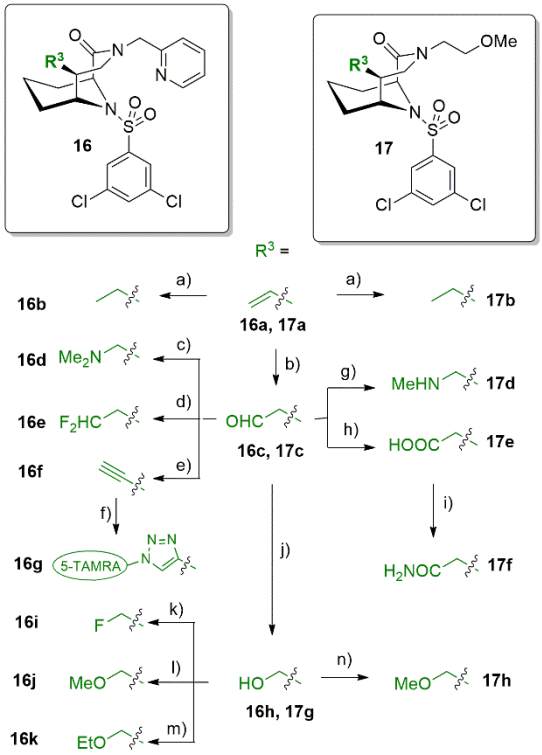

Figure 3. Derivatization of the R^3-position. Reagents and conditions: a) Pd/C, H_2, MeOH, rt, 12 h, 16b: quant., 17b: quant.; b) OsO_4, $NaIO_4$, Lutidine, Dioxane/H_2O, rt, 20 h, 16c: 60 %, 17c: 70 % c) $NHMe_2$, $NaBH_4$, MeOH, 24 h, rt, 35 %; d) DAST, CH_2Cl_2, rt, 2 h, 67 %;e) Ohira-Bestmann-Reagent, K_2CO_3, MeOH, rt, 2 h, 53 %; f) 5-TAMRA-Azide, TBTA, Na-ascorbate, $CuSO_4$, *t*-BuOH/H_2O, 6 h, 37 °C, 27 %.g) NH_2Me HCl, $NaBH(OAc)_3$, MeOH/AcOH, rt, 4 h, 33%; h) Methylbutene, $NaClO_2$, NaH_2PO_4, $CHCl_3$/t-BuOH/H_2O, rt, 16 h, 93 %; i) CDI, NH_3, EtOAc, rt, 2 h, 41%; j) $NaBH_4$, EtOH, rt, 1 h, 12h: quant. 17g: 65 %; k) DAST, CH_2Cl_2, rt, 1 h, 52 %, l) NaH, MeI, THF, 0°C - rt, 1 h, 16j: 59%, 17h: 50%; m) NaH, EtI, THF, 0°C - rt, 1 h, 50%.

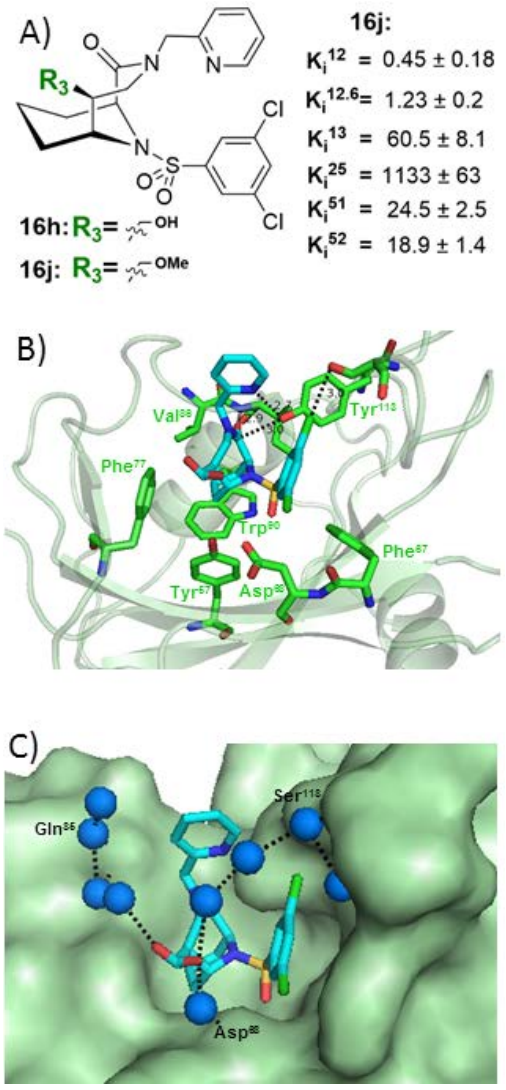

Figure 4. A) Chemical structure of the universal FKBP inhibitors **16h** and **16j** and the affinities of **16j** to human FKBPs (K_i in nM). **B)** Cocrystal structure of **16h** (shown in cyan) in complex with the FK506-binding domain of FKBP51 (pale green cartoon) with key residues shown as green sticks. The main interactions of R^1, R^2 and R^3 with FKBP51 are shown as black dashed lines (pdb code: 5OBK). **C)** Cocrystal structure of **16h** as in B) with FKBP51 shown as pale green surface**.** The water network engaged by the C^5 CH_2OH group is highlighted as blue spheres and black dotted lines.

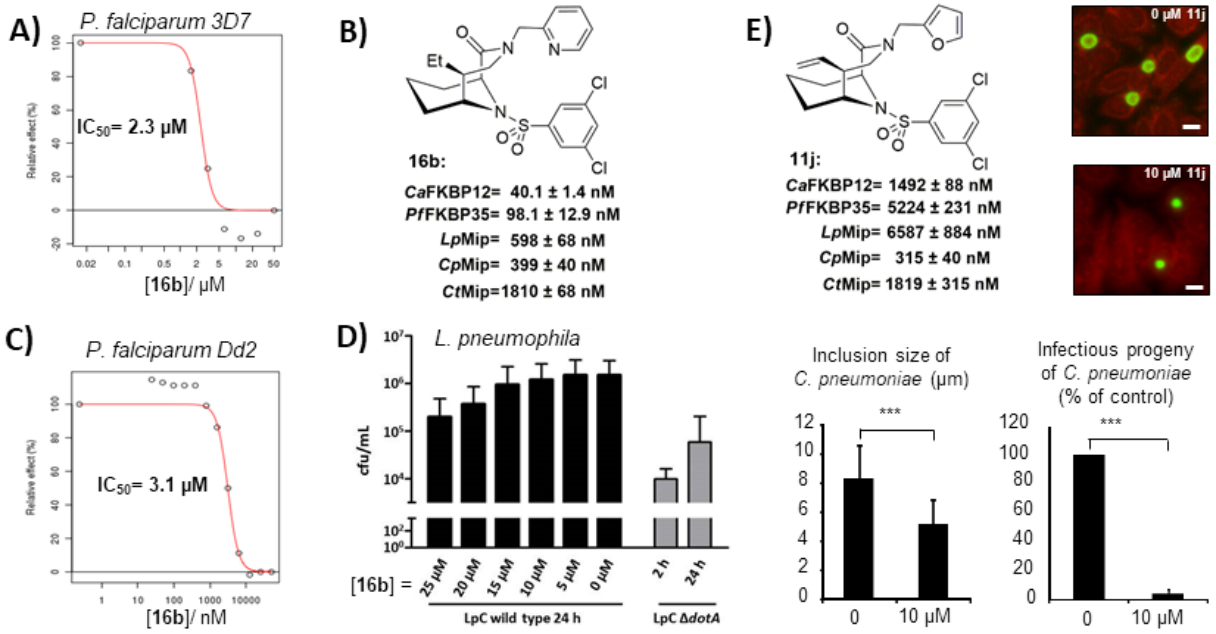

Figure 5. Antimicrobial activity of bicyclic FKBP/Mip inhibitors. **A) 16b** inhibits the growth of the *P. falciparum* strain 3D7 strain in a dose response manner. Parasite viability was measured by FACS reading of Hoechst 33342 stained cultures following a complete life cycle incubation with the compound. **B)** Chemical structure and biochemical activity of compound **16b**. **C)** Compound **16b** retains growth inhibition in the multidrug-resistant *P. falciparum* strain Dd2. **D)** Compound **16b** inhibits intracellular proliferation of *L. pneumophila* in a dose dependent manner. Shown are the cfu/ml 24 hpi. Wild type *L. pneumophila* strain Corby (LpC) in the presence of DMSO only were used as positive control while the avirulent *dotA*-deficient strain served as a negative control. The graph depicts the means and standard deviations of three independent experiments performed in duplicate. **E)** Effect of **11j** on primary infection (bottom left, n=40, 40 chlamydial inclusions from 4 independent experiments were measured) and on infectious progeny of *C. pneumoniae* (bottom right, n=3, Mean ± SD, Student's *t*-test, ***$p \leq 0.001$]). Infectious progeny of *C. pneumoniae* were analyzed by a recovery assay (right, scale bar = 10 µm) by staining chlamydial inclusions (green) and host cells (red).

Table of content graphic